Library

UHF COMMUNICATIONS SATELLITE SYSTEM

FINAL REPORT/VOLUME II

RCA Space Systems

LKC
P
91
.C654
U35
1971
v.2

IC

RCA LIMITED
1001 Lenoir St., Montreal 207, Canada

COMMUNICATIONS CANADA
JUIN JUNE 7 1984
LIBRARY – BIBLIOTHÈQUE

Industry Canada
Library - Queen
AOUT AUG 16 2012
Industrie Canada
Bibliothèque - Queen

UHF COMMUNICATIONS SATELLITE SYSTEM

FINAL REPORT/VOLUME II

The work reported here was done under DDS Contract OPL1-0005 "Consulting Services for Cost Studies of UHF Satellite Communications Systems" and under the design authority of the Communications Research Center of the Department of Communications.

Prepared by:

Government and Commercial Systems Division,
RCA Limited, Ste. Anne de Bellevue, Quebec

Project: 2217-0

December 9, 1971

P
91
C654
U335
1971
v.2

DD499700
DL 449744

TABLE OF CONTENTS

TABLE OF CONTENTS (continued)

LIST OF FIGURES

LIST OF TABLES

1. SPACECRAFT PERFORMANCE REQUIREMENTS

The spacecraft characteristics are summarized in Tables 1.1 and 1.2 for the two frequency assignments, with the resulting designs illustrated in Figures 1.1 and 1.2. These specifications and designs are in response to the System Traffic Model as stated in the Requirements Document as developed within the framework of system and space segment trade-offs discussed in Volume I.

The following sections of this volume discuss in more detail the subsystem alternatives and resulting subsystem performance specifications.

TABLE 1.1 - Spacecraft System Characteristics

Three Axis Stabilized Spacecraft	
Size	Height 46", Diameter 71" × 55"
Weight	1500 lbs (including 76.6 lbs margin)
Communications	300-400 MHz Transponder - Single Channel Multiple Access: 100 duplex, 5 simplex, EIRP: 41.2 dBW G/T: -11.0 dB
Coverage	All of Canada
Stabilization	Double Gimballed Reaction Wheel
Attitude Control Sensor	Static Earth Sensor
North South Inclination Control	None
Power	Flexible Solar Sails with 2 Batteries giving 14% Eclipse Capability
Telemetry	PM/PCM
Command	PCM/FSK/AM
Lifetime	5 years
Reliability	.695

RCA

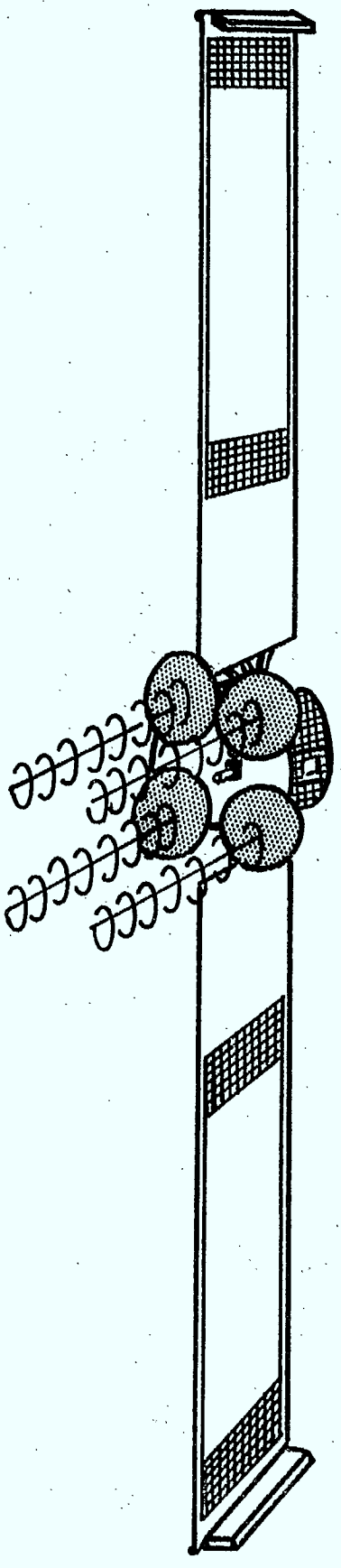

TABLE 1.2 - Spacecraft System Characteristics

Spin Stabilized Configuration	
Size	Height 55", Diameter 86"
Weight	1500 lbs (including 118.5 lbs margin)
Communications	1.5 GHz Transponder - Single Channel Multiple Access: 100 duplex, 5 simplex, EIRP: 37.5 dBW G/T : -2.4 dB
Coverage	All of Canada
Stabilization	Dual Spin - Favourable Moment of Inertia Ratio
Attitude Control Sensor	Spinning Earth Sensor
North South Inclination Control	Yes
Power	Body Array with 2 Batteries giving full Eclipse Capability
Telemetry	PM/PCM
Command	PCM/FSK/AM
Lifetime	8 years
Reliability	.660

RCA

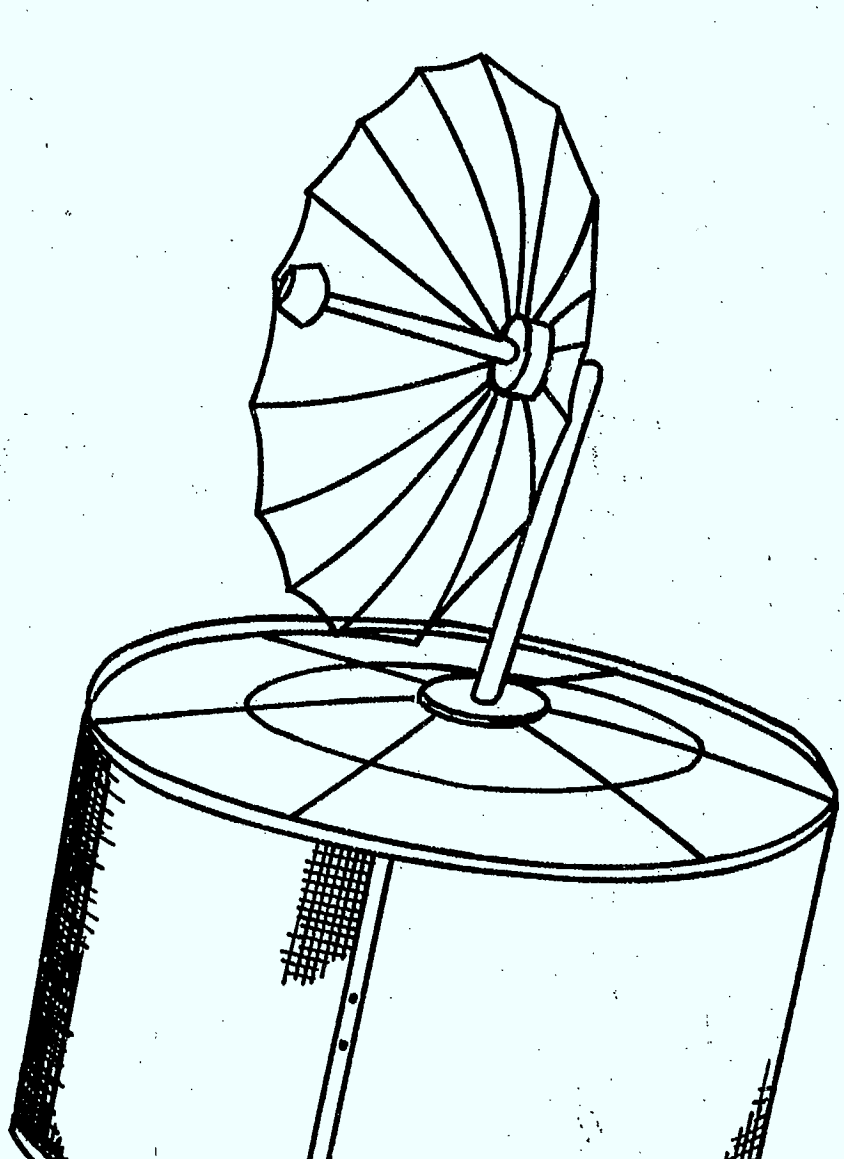

2. ANTENNA DESIGN

2.1 Introduction

This section describes the trade-offs and outlines the design approach for the proposed antenna subsystems, examining the single element end-fire antenna, arrays of high gain end-fire elements, electrically despun antennas, and circular aperture paraboloids. In all cases, including the 1.5 GHz systems, the antennas are circularly polarized to avoid Faraday rotation effects, with no cross-polarization for up- and down-links. It is expected that no difficulty will be experienced in providing an ellipticity within the coverage circle of less than 2 dB. It is convenient here to note that the preferred choices of antenna for the two frequency bands are

300 MHz	3-Axis Stabilized:	Deployable Quad-Helix
1.5 GHz	Spin Stabilized:	Deployable Paraboloid (Umbrella type)

The principal problem in designing the antenna subsystem for a communications satellite is usually one of maximizing the equivalent isotropically radiated power, carrying with it the implied problems of maximizing the communications antenna gain and minimizing antenna weight. For practical systems, the maximum gain that can be achieved over a given coverage area is determined not by the size of the antenna's aperture but by the coverage requirement itself. In other words, in a practical case where diameter is limited for various reasons, no class of aperture distribution is capable of increasing the off-axis gain over that achieved with an optimum simple tapered aperture distribution. An increase in aperture diameter over the minimum required to give a 3 dB beamwidth corresponding to the required coverage can yield increased off-axis gain if sophisticated aperture distributions are used, but

there are important practical obstacles which militate against this approach. No proof of this as yet exists, though Rebhan[1] has shown that, for a circular aperture, the optimum aperture illumination to yield a maximum value of off-axis antenna gain is $J_o(r)$. His analysis is inadequate for off-axis gains between his $J_o(r)$ results and the maximum sector pattern gain achievable from an infinite $J_1(r)/r$ class of aperture illumination. Holland[2] has shown that the off-axis gain achievable from a $J_o(r)$ aperture illumination is almost indistinguishable from that from a wide variety of different distributions. Holland speculates that higher gains, up to the sector gain limit, are not physically realizable without unrealistically large apertures. He also makes the observation that so-called beam-shaping techniques are not worthwhile from the point of view of increasing edge gain for diameter-limited antennas, but are very useful in decreasing off-axis gain slope and hence the susceptibility of the communications antenna gain to spacecraft pointing errors.

In order to realize improvements in edge gain from circular apertures, circularly symmetric illumination functions should be used. The illumination from most practical feeds is separable so that the necessary symmetry cannot be achieved. When the antenna is diameter-limited sophisticated feed systems or reflector-stepping techniques can be used but are not capable of increasing edge gain above that achievable from an aperture of the same diameter with a simple tapered aperture illumination.

In determining the coverage area required for a spacecraft antenna with a given pointing error (say $\pm \Delta$ degrees), it is usually sufficient to determine the coverage required by an error-free spacecraft, say $\pm \theta$ degrees, and to take the coverage requirement as $2(\Delta + \theta)$ degrees. The antenna must

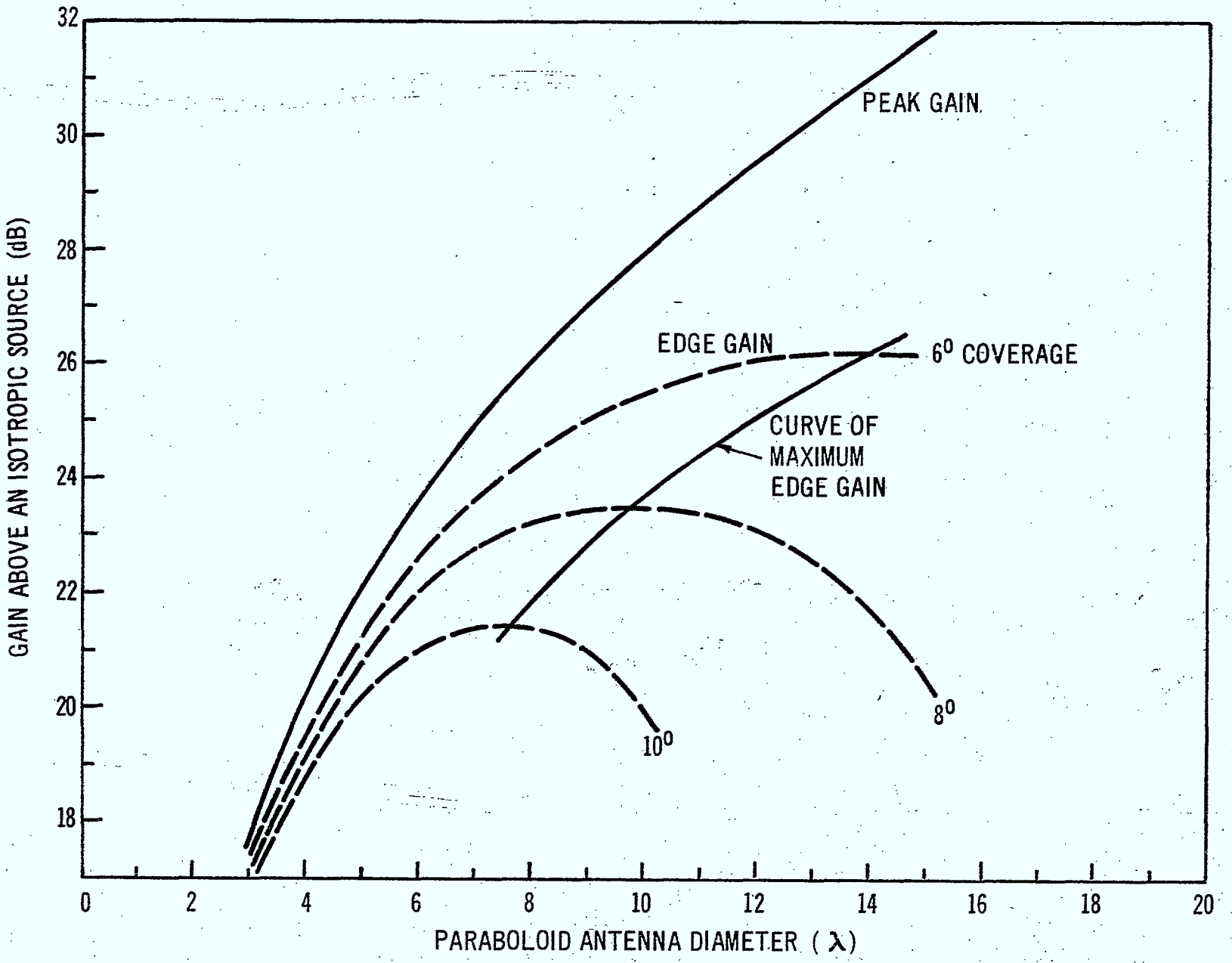

Figure 2.1 – Peak Gain and Edge Gain Variation with Paraboloid Diameter

then be designed to give adequate gain at $\Delta + \theta$ degrees off-axis. By making some simplifying assumptions it is therefore possible to determine the relationship between off-axis gain, antenna size and coverage. The 3 dB beamwidth of an optimally illuminated circular objective is given by[3]

$$\theta_{3dB} = 65.9 \frac{\lambda}{D} \text{ degrees} \qquad (2.1)$$

Assuming a parabolic relationship between the decibel power level and off-axis angle θ, it is then easy to calculate the off-axis loss in gain. Next, applying the commonly used expression for antenna peak gain

$$G = \frac{27,000}{\theta^2_{3dB}} \qquad (2.2)$$

it is possible to construct Figure 2.1. This diagram shows firstly (upper solid line) the practical (i.e. including spillover, illumination, phase error and thermal losses) maximum gain obtainable from a circular aperture. Secondly, the dashed lines show the practical off-axis, or edge of cover, gains as a function of antenna diameter. The maximum edge of cover gain is shown by the lower solid line. Thus, if the coverage requirement is an 8° circle, the maximum practical edge gain is 23.5 dB. This figure will be found to differ slightly from later calculations of edge gain, the difference being due to the assumptions made in the choice of the gain constant 27,000 in (2.2).

These results are cross-plotted on Figure 2.2, which shows the maximum edge gain as a function of coverage circle diameter. Taking again the previous 8° circle as an example, other edge gains for elliptical beams can be deduced. Thus a $4^\circ \times 8^\circ$ beam would yield a 3 dB increase in edge gain to 26.5 dB, whilst a $3^\circ \times 9^\circ$ beam would provide a further .74 dB improvement to 27.24 dB. Again these simplistic calculations differ slightly from practical results for the previously stated reasons.

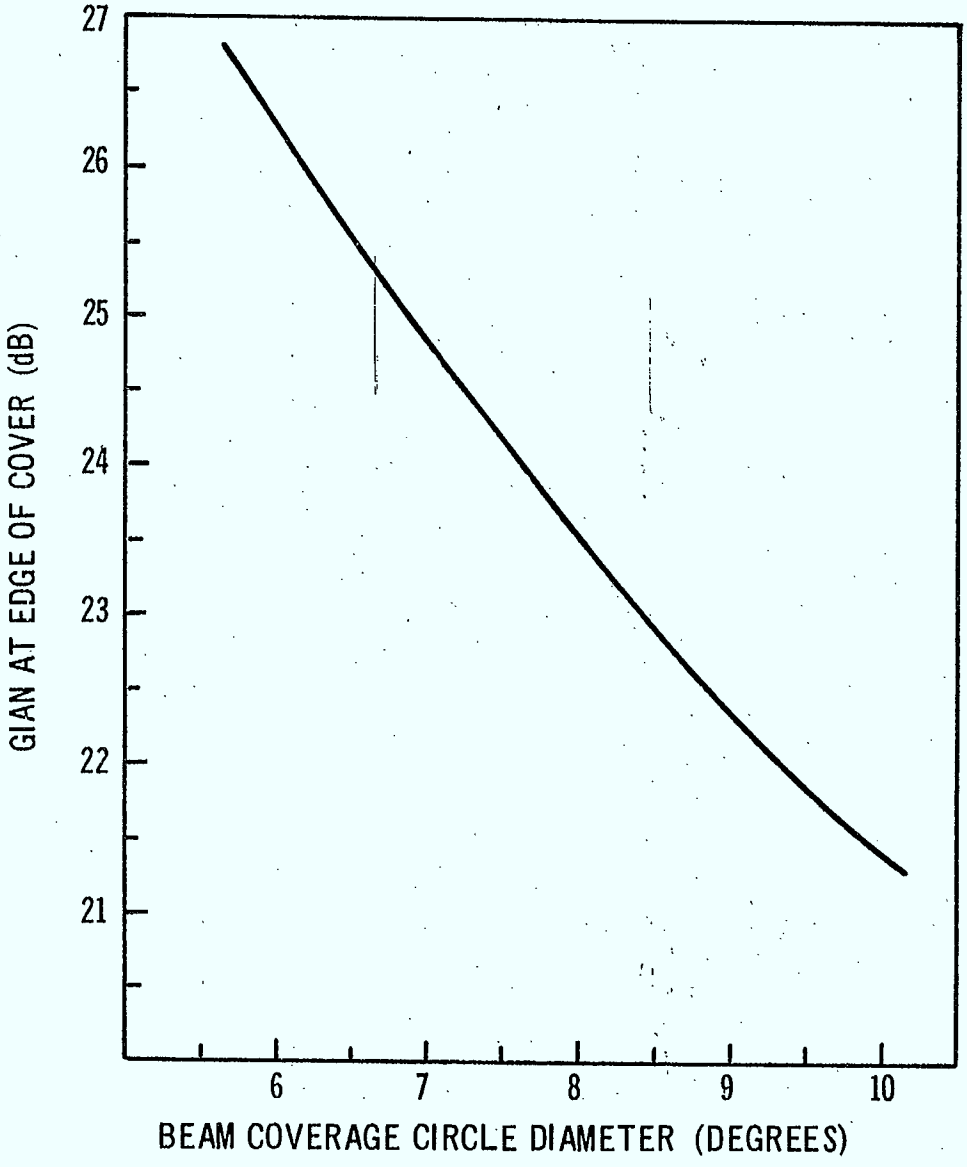

Figure 2.2 – Maximum Edge Gain as a Function of Coverage Diameter

In the present proposal the antenna designs are concerned with two frequencies, 1.5 GHz and 300 MHz, with wavelengths of 8 inches and 40 inches respectively. Taking Canadian coverage, somewhat arbitrarily, as an 8 degree circle, maximum edge gain requires aperture diameter of 9.75 λ (see Figure 2.1) or 78 inches and 390 inches respectively. It is clear that considerable weight penalties are carried by the 300 MHz design and some compromise must be made between edge gain and aperture size. Thus, if an edge gain of 18.7 dB is acceptable, the aperture diameter at 300 MHz may be reduced to 3.8 λ or 152 inches. However, it is no longer certain that a circular aperture would provide the optimum antenna. Other considerations such as spacecraft type, whether 3-axis or spin stabilized, must be taken into account.

Techniques used in other spacecraft show that a common choice for a VHF or UHF communications satellite antenna is a spin stabilized configuration with a deployable end-fire array where high gain (18 dB) is required (for example TACSAT) or where moderate gain (8 dB) is required, with an electrically switched array (for example LES-6).

2.2 End-Fire Antennas

2.2.1 Single Element

End-fire antennas such as the Yagi or helix provide convenient elements for deployable antennas at VHF or UHF wavelengths and it is relatively easy to incorporate circular polarization. However, while the helix is naturally circularly polarized, the Yagi requires, in effect, a double array. Furthermore, the Yagi is bandwidth limited in comparison with the helix. Also the helix is probably a little easier to deploy (as a spring, for example) than the Yagi. For these reasons, the helix is chosen as the end-fire element.

Although the end-fire element causes no shadowing of the solar sails on a 3-axis stabilized spacecraft during the equinoxes, in this respect being superior to planar or reflector antennas, the end-fire element will cause shadowing (defined by the geometry of Figure 2.3) at solstice. Thus, for d = 30 inches in Figure 2.3, the maximum length of a single end-fire element is 69 inches. The approximately equivalently shadowing diameter of a circular reflector is 2 × d + 12" or 72 inches. At 300 MHz the equivalent peak gains may be calculated to be 12.3 dB for the helix and 13 dB for the circular reflector, neglecting feed blockage. Hence, the shadowing problems are roughly comparable.

The 3 dB beamwidth of a helix of length L wavelengths is given by Kraus[4] as

$$BW = \frac{52}{\sqrt{L}} \text{ degrees} \qquad (2.3)$$

where the helix circumference is approximately 1 wavelength and the pitch angle is approximately 15°. This is plotted in Figure 2.4 as a function of L. Kraus also gives gain as

$$\text{Gain} = 15L \qquad (2.4)$$

but this formula is based on solid angle considerations only and neglects beam taper and sidelobes. Again, a more realistic expression for gain is given by Eq. (2.2) which, together with Eq. (2.4), are also plotted in Figure 2.4.

A weight estimate for a deployable single element helix antenna on a 3-axis stabilized spacecraft has been made assuming a STEM central erection member. The helix has been taken as a partially self-erecting spring with

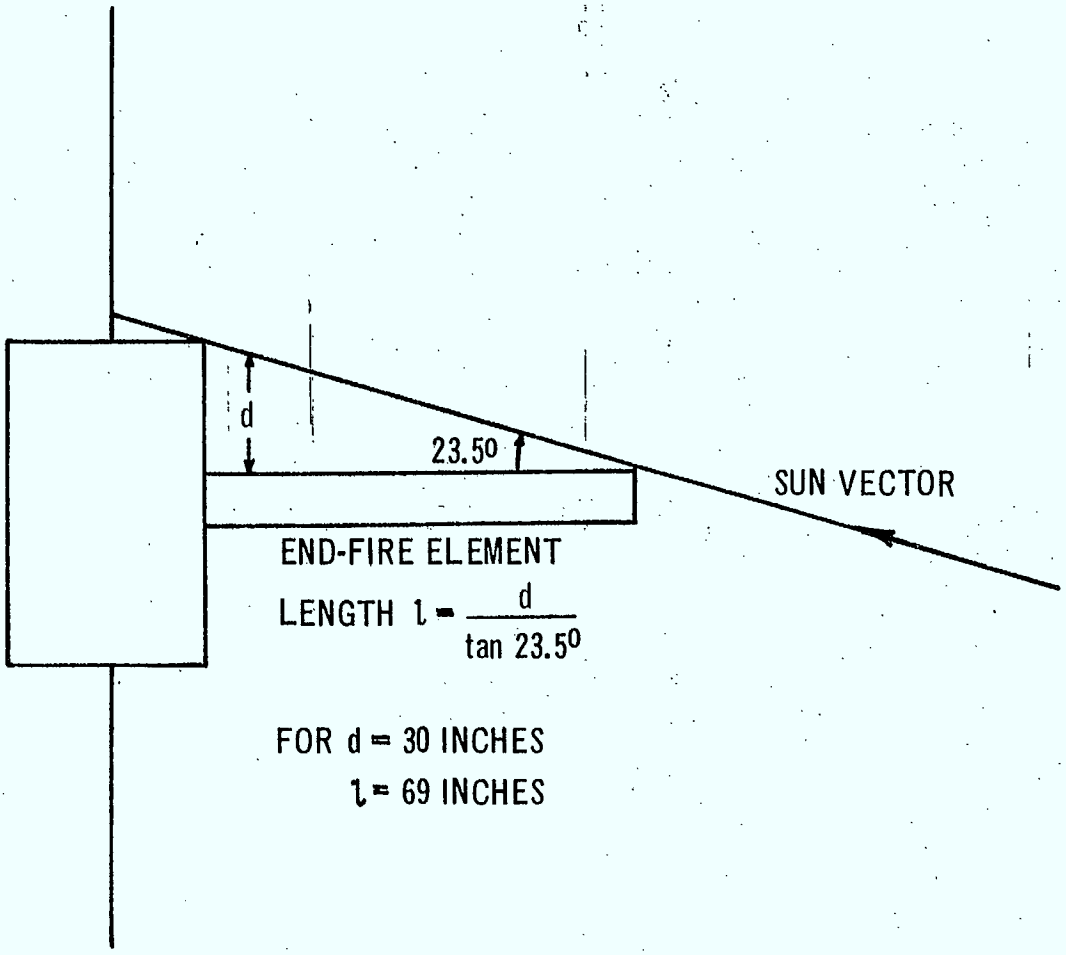

Figure 2.3 – Solstice Shadowing of Solar Sails by a Single Element at 300 MHz

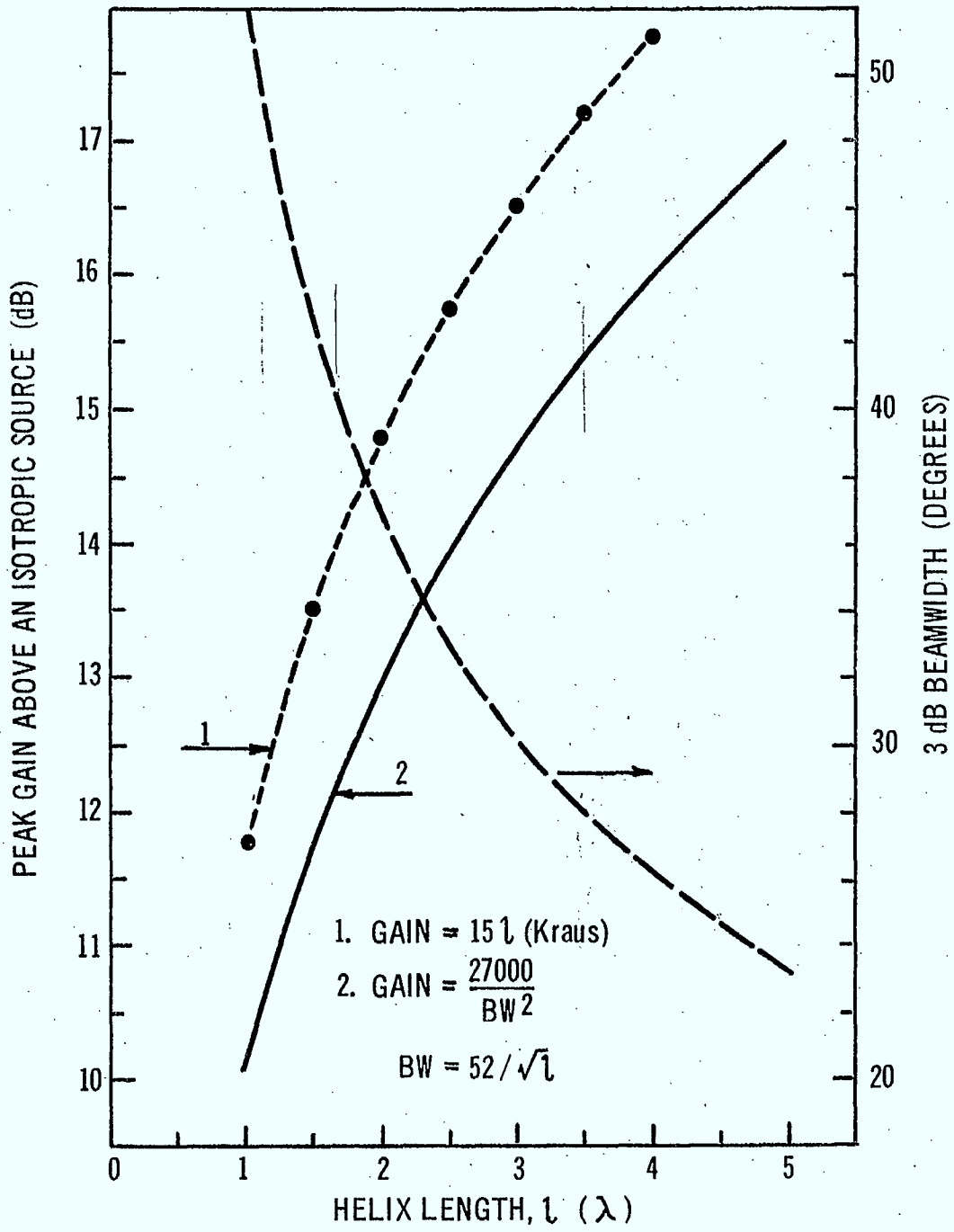

Figure 2.4 – Single Helix Gain & Beamwidth

ground plane integral with the forward equipment platform. A minimum weight of around 6 lbs for the STEM, ground plane, dielectric supports and stowage canister gives a weight of 7.5 lbs for a 40 inch helix at 300 MHz. The variation in weight is plotted in Figure 2.5 together with the gain at edge of Canadian coverage, defined here as a 10 degree circle.

These curves are cross-plotted onto Figure 2.16 to show the gain-weight relationship for different antenna concepts. It will be noted that the single helix antenna offers a clear advantage for a 3-axis stabilized spacecraft at 300 MHz, for moderate gains. However, the efficiency of the helix is likely to decrease as its length is increased, resulting in a levelling-off of the gain-weight curve.

2.2.2 Quad-Helix Arrays

In order to obtain higher gain without increasing the length of the single helix, helices of moderate length may be combined in arrays, of which the quad-helix array is a good example. Figure 2.6 shows the variation of array peak gain as a function of element spacing S in wavelengths for arbitrary elements. A range of element gains is shown. Cross-coupling and mismatch losses are neglected. In each case the peak gain is 6 dB above the element gain at the optimum spacing. Using Eq. (2.2), the 3 dB beamwidth of the quad-helix array can be estimated, shown in Figure 2.7, as a function of helix axial length.

Little data is available on the weight of deployable despun quad-helix arrays. However, a Hughes Aircraft Company study[5] of a 150 MHz, 20 inch diameter element, quad-helix array indicates a weight of 62.5 lbs for 200 inch

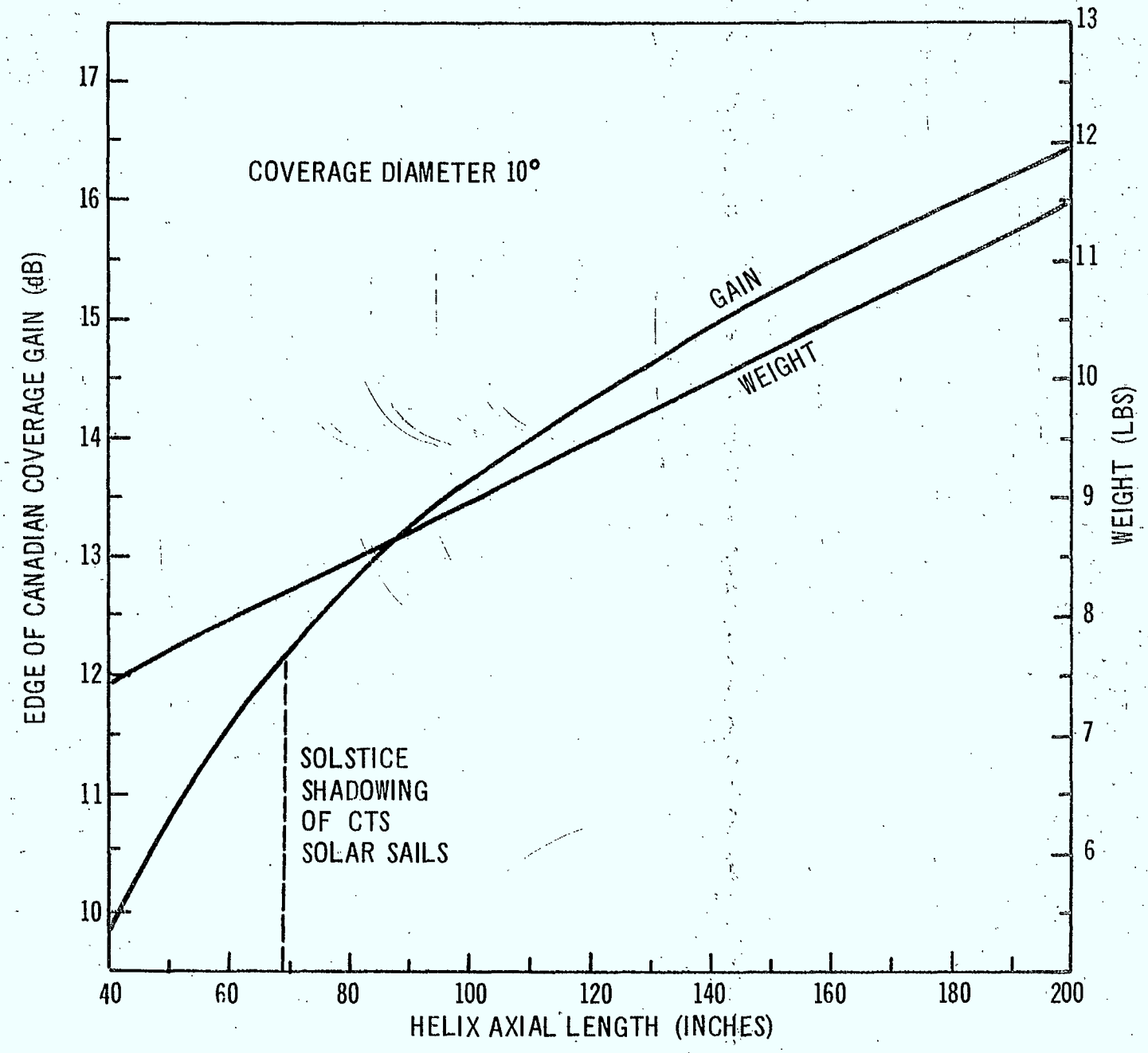

Figure 2.5 – Gain, Weight & Length for 300 MHz Deployable Single Helix Antenna – 3-Axis Stable

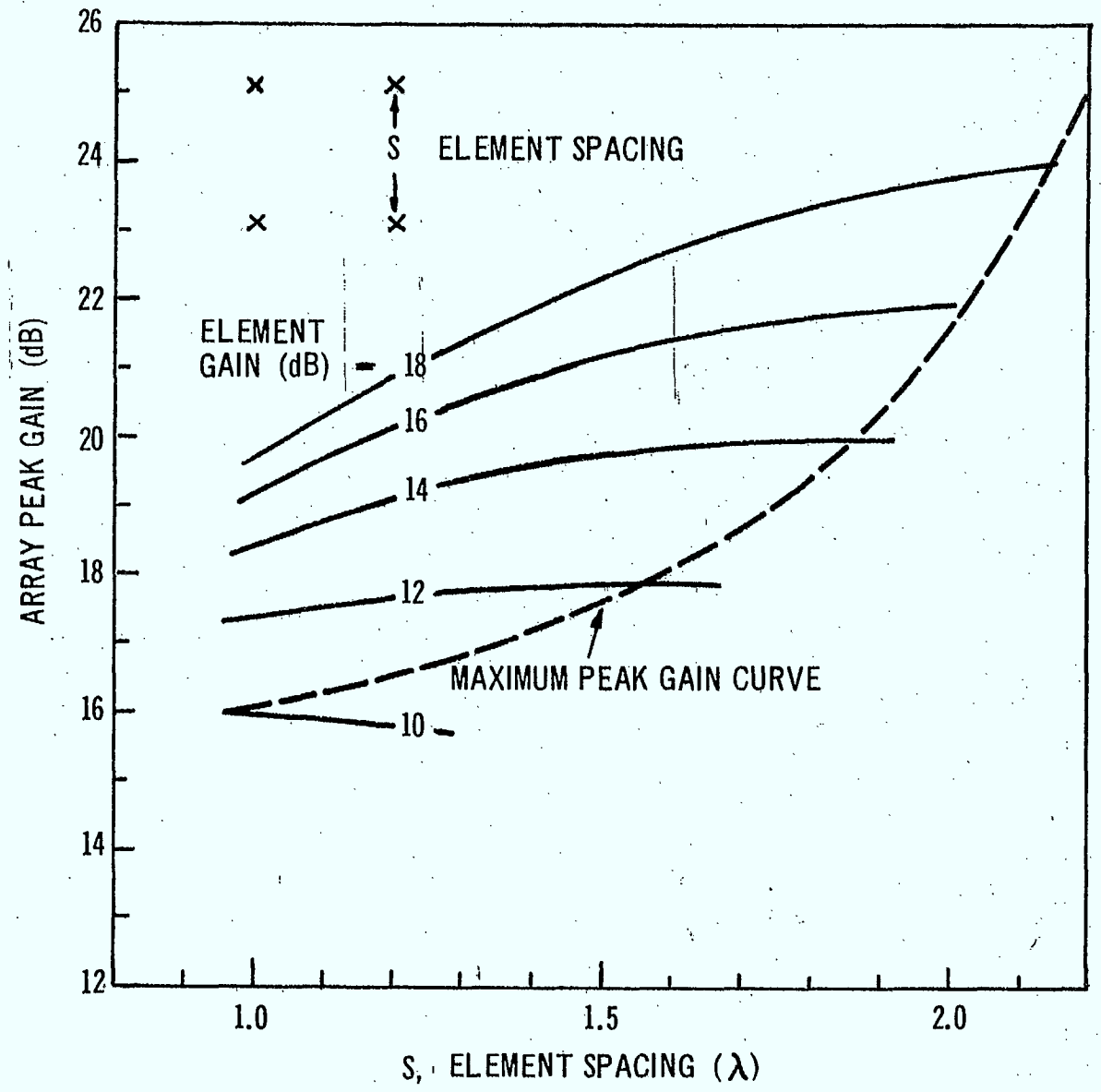

Figure 2.6 – Array Gain Peak versus Element Spacing for Different Element Gains

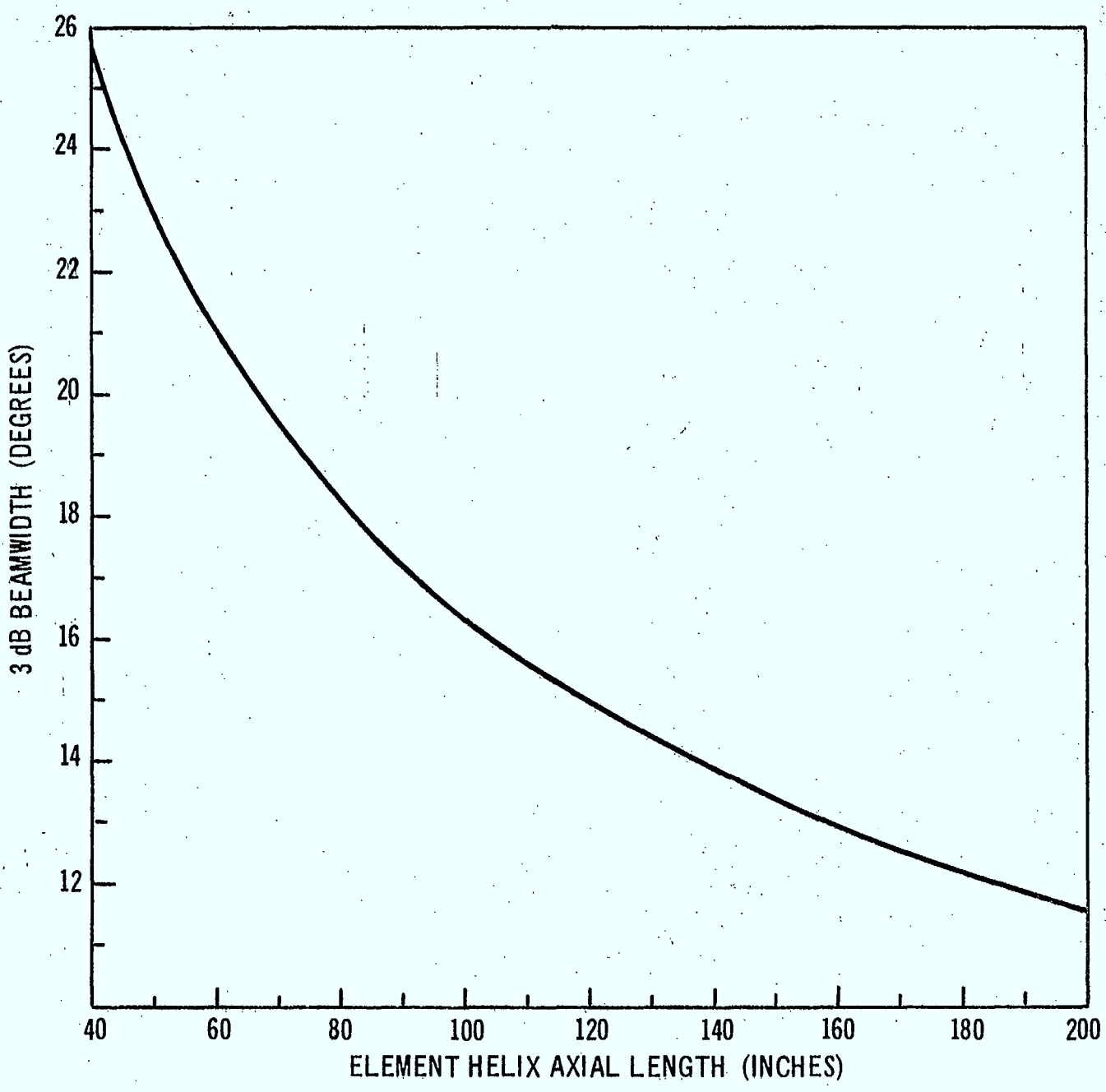

Figure 2.7 – 3 dB Beamwidth of Maxiumum Gain Quad-Helix Array – 300 MHz

long elements. Using this as a starting point, it is assumed that a 200 inch long quad-helix array at 300 MHz will have the same element spacing in inches (due to the higher element gain) and hence essentially the same deployment mechanism. Offsetting this, the helix-diameter will be 12 inches thus yielding a slightly lower weight, or 60 lbs. Rough estimates of the weight of a 40 inch helix have been made and the two extreme points connected by a straight line. This is shown in Figure 2.8. Also shown are the element peak gain and the edge of Canadian coverage gain, here taken as a 10° circle, for a 300 MHz spin stabilized spacecraft.

A cross-plot showing the gain-weight relation is given in Figure 2.15.

2.3 Electrically Despun Antennas

Two techniques are available for electrically despinning a circular array. One uses phasing networks which set up an appropriate wavefront from all available elements of a circular array. This involves heavy and complex RF circuitry of variable phase shifters. The other uses simple switching networks, incorporating devices such as PIN diodes. A typical example of the second approach is the LES-6 antenna consisting of two circular arrays, each of 8 circularly polarized elements, stacked along the spin axis. By switching from three to four to three, etc., elements, progressing around the circumference, sixteen overlapping beams are generated. Since the elements are spaced at half-wavelength intervals around the spacecraft, and the spacecraft diameter is about 1.3 wavelength, the equatorial plane beamwidth is about 50°, actually 54° [6]. No phasing networks are used, all elements being fed in phase. There is accordingly a limit on the number of elements which can be fed in this

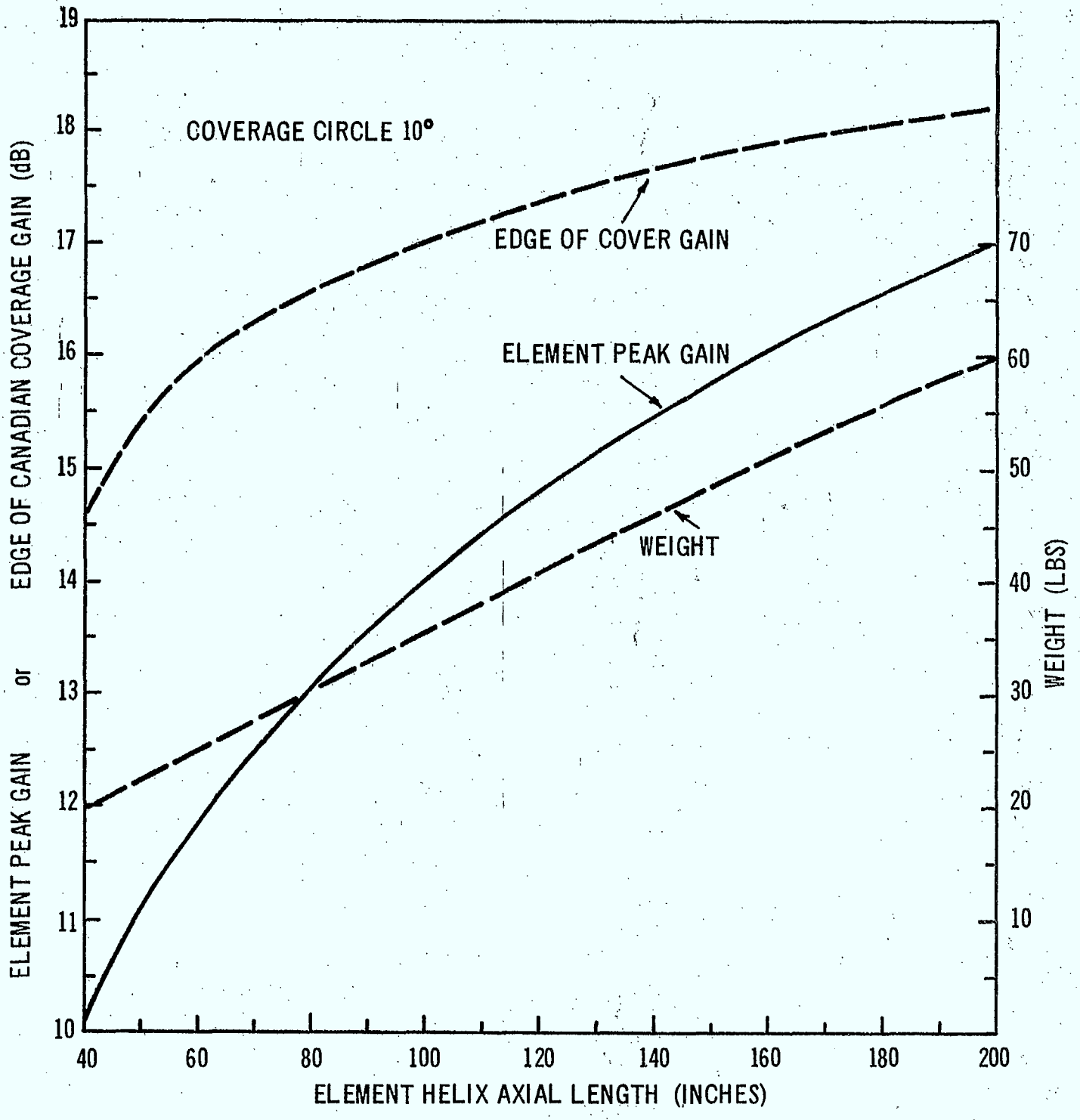

Figure 2.8 – Gain, Weight, Length of 300 MHz Deployable Quad-Helix Array Antennas – Spin Stabilized

manner, since phase error effects become otherwise pronounced. Similarly, the element-to-element separation cannot be allowed to exceed greatly a half-wavelength. Thus at 300 MHz on a 6 ft diameter spacecraft a minimum of 11 elements would be required, nevertheless capable of forming only a 35° E-W beam. On the other hand, at 1.5 GHz on a 6 ft diameter spacecraft, 55 elements would be needed, but only a limited group of perhaps 5 elements could be excited. The E-W beamwidth would hence still be around 35°. Further improvements in gain must therefore be achieved by stacking the circular arrays along the spin axis. Thus, LES-6 yields approximately 8.5 dB gain from a double stacked array. 11.5 dB requires a further two circular arrays, 14.5 dB a further four, and so on.

Using the weight estimate of 5 lbs for an 8 dB gain electrically switched array described by Kiesling and Maco,[7] an estimate of 14 lbs for an 11 dB gain four circular array system has been deduced. This figure assumes an arithmetic doubling of weight (2 × 5 lbs) plus a 40% allowance (4 lbs) for supporting structure (it is possible that such an antenna would not need to be deployable). Any further increase in gain would probably require a deployable concept and the gain-weight relation plotted in Figure 2.15 would tend to flatten.

2.4 Deployable Paraboloid Antennas

2.4.1 General

Deployable paraboloid antennas for spacecraft have been proposed and in some instances built though their diameters have not been great. In particular, RCA Corporation has built two unbrella-type antennas for the Apollo program. Both of these were manually erected on the lunar surface and have thus been space qualified.

An important consideration is the weight-diameter relation of erectable paraboloids. Using the precise RCA data from the Apollo antennas and an RCA estimate for a 75 ft diameter antenna built on similar lines, Figure 2.9 has been plotted on log-log paper. It may be noted that the RCA weight figures include the feed support and feed line contributions. Millikin[8] of Hughes Aircraft Co. has published results of a comparative study of different deployment techniques which show that the umbrella type offers the lowest weight. His results are also plotted in Figure 2.9.

A straight line has been drawn to provide a basis for weight analysis of the proposed antenna.

2.4.2 Aperture Blockage

It has been observed in Section 1 that in the present application aperture sizes in the range 3.8 λ to 10 λ are required. Now typical reflector feed systems have gain, G_o, between 6 dB and 8 dB: the effective feed capture area is then given by

$$A = \frac{\lambda^2}{4\pi} \cdot \text{antilog}_{10}\left(\frac{G_o}{10}\right)$$

or

$$A = \frac{\lambda^2}{4\pi} \cdot G, \quad G \text{ is numeric gain.}$$

Hence the blocking obstacle diameter is given by

$$D = \frac{\lambda}{\pi}\sqrt{G}$$

For G_o = 6 dB, which might be a typical value for a dipole/reflector feed for 300 MHz, $D = .64\,\lambda$. For $G_o = 8$ dB, $D = .8\,\lambda$. Thus in a 3.8 λ aperture, the ratio of blocking obstacle diameter to aperture diameter may range between

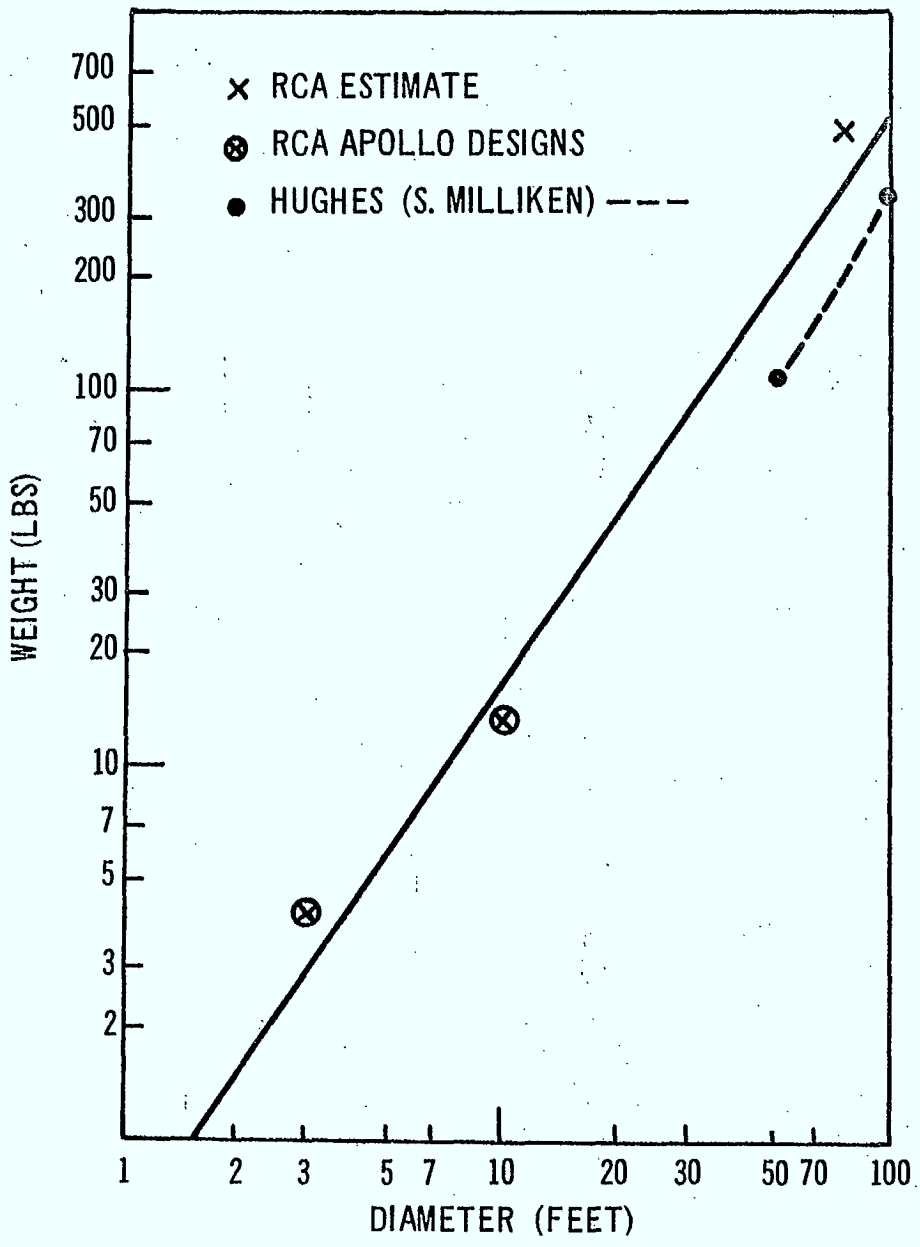

Figure 2.9 – Weight-Diameter for Deployable (Umbrella class) Paraboloid Antennas

.17 and .21 causing a substantial gain loss.

Aperture blockage effects have been computed for a circular aperture with central circular obstacles for a range of blockage ratios and a range of simple aperture distributions of the form $(1-r^2)^N$, with N = 0,1 and 2. These results are shown in Figures 2.10, 2.11 and 2.12. Figure 2.10 demonstrates the significant beam narrowing, and hence increased gain slope, due to blockage. As expected the first sidelobe level increases until, for large blockage ratios, the annular aperture distributions are not significantly different to cause great variations in sidelobe level. Figure 2.11 plots the two contributions to blockage loss, the change in aperture efficiency η_B and the fractional power scattered by the obstacle P_B. The total gain loss, normalized to the maximum is given by

$$\text{Gain Loss} = -10 \log_{10} \left[\eta_B (1 - P_B) / \eta_{B_{d=0}} \right]$$

and is plotted in Figure 1.12.

Taking N = 1 as a typical distribution, the gain loss for a blockage ratio of .2 is 0.7 dB with a 5% reduction in beamwidth. These results have been used in calculating the gain performance of paraboloid antennas in the following sections.

2.4.3 300 MHz Deployable Paraboloids

2.4.3.1 Gain

The edge of cover gain with coverage defined as a 10° circle has been calculated for a range of diameters from 100 to 400 inches. It has been assumed

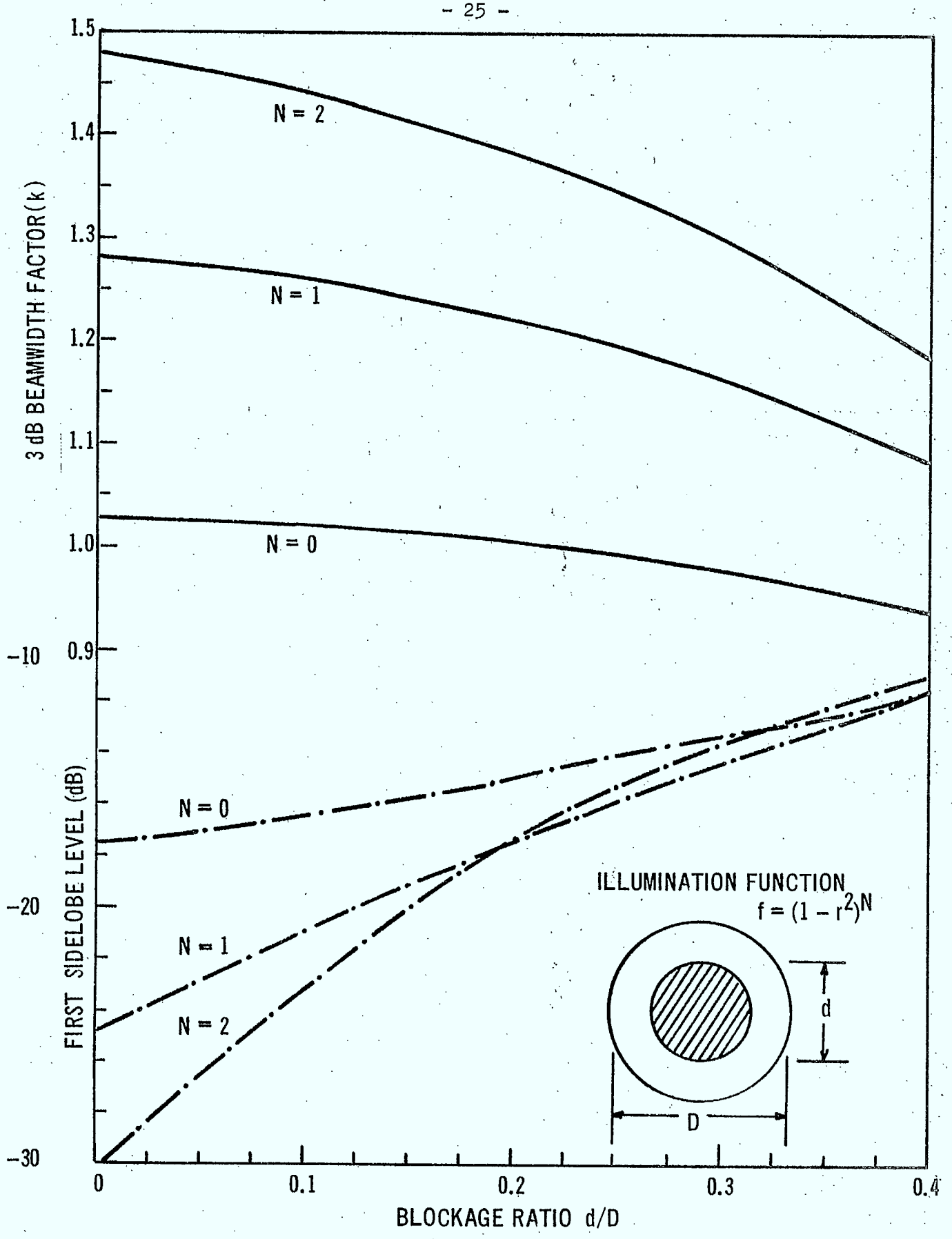

Figure 2.10 – Beamwidth and Sidelobe Effects due to a Central Obstacle

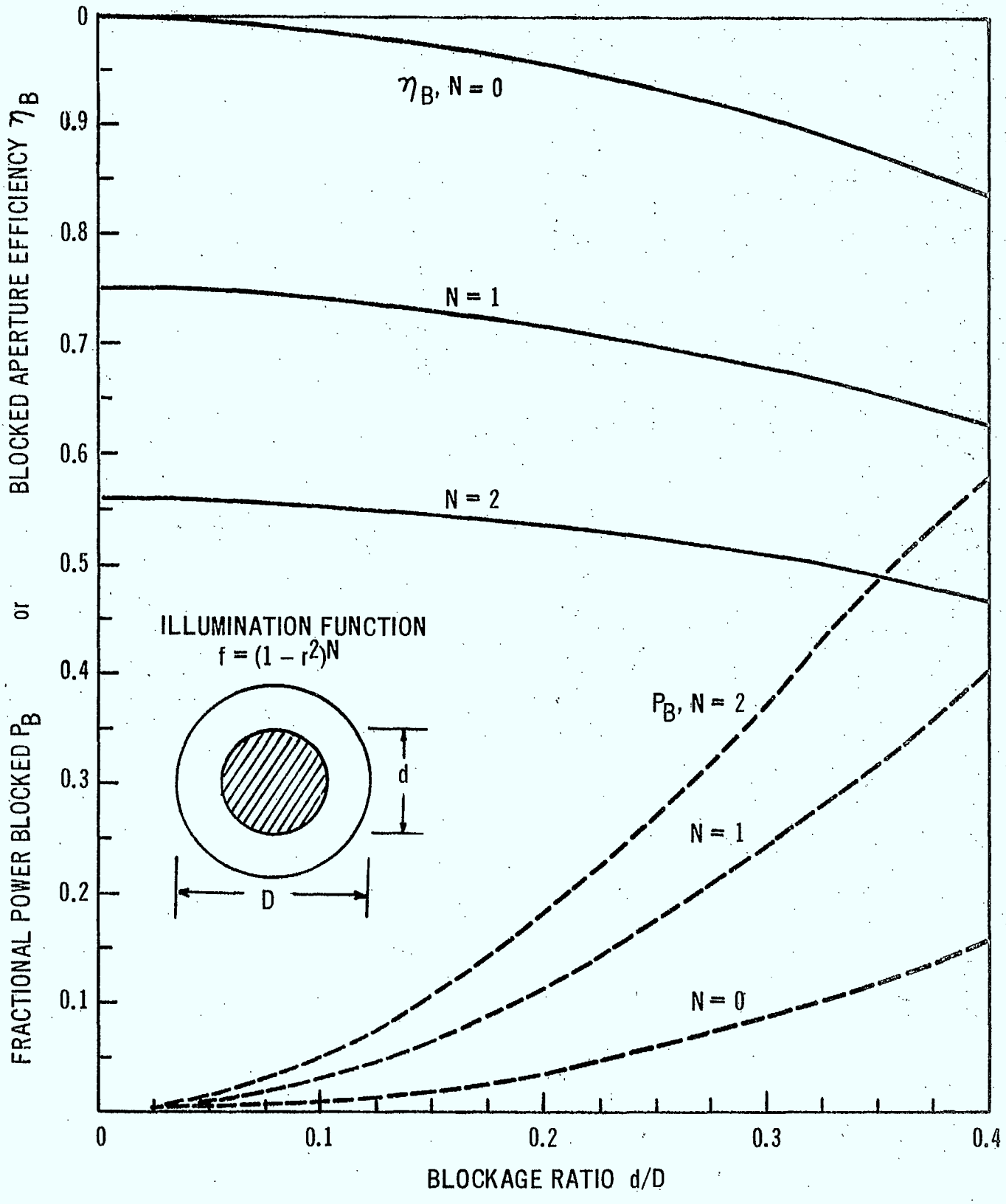

Figure 2.11 – Aperture Efficiency and Blocked Power due to a Central Obstacle

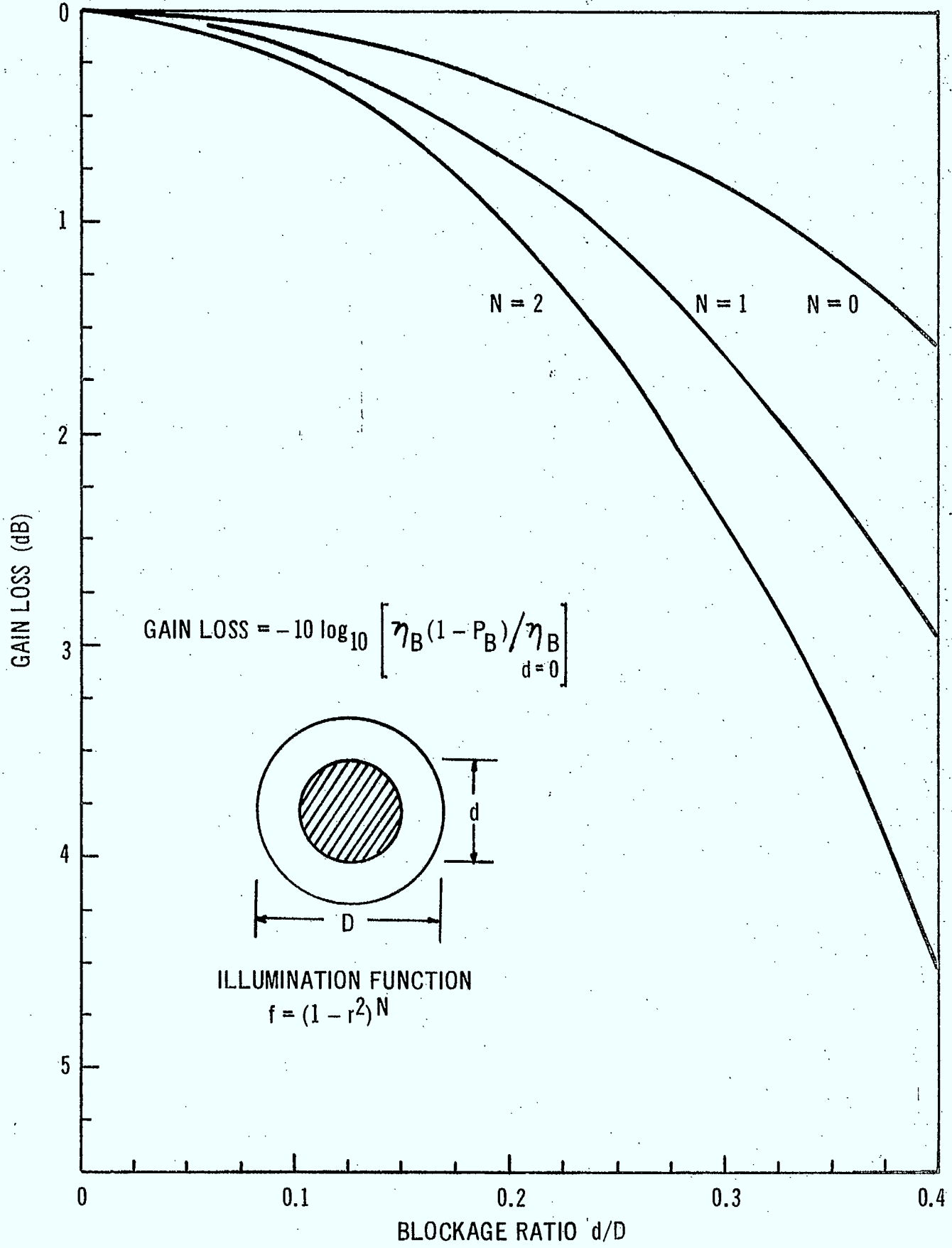

Figure 2.12 – Gain Loss due to a Central Obstacle

that the feed is a dipole/reflector combination with a gain of 6 dB, that the f/D of the reflector is about 0.25 and that the feeder cable follows a maximum length route consisting of half the diameter, the focal length plus 3 ft of spare. A simple parabolic (N = 1) illumination function has been used. Blockage effects on peak gain and gain slope have been included.

The variation with diameter is plotted in Figures 2.13 and 2.14. The maximum gain is 21.1 dB, which for an 8^{o} coverage circle would improve to approximately 23 dB. This somewhat low figure (by about 0.5 dB) is due to pessimistic assumptions on spillover.

2.4.3.2 Antenna Weight - Spin Stabilized Spacecraft

The straight line of Figure 2.9 has been used to calculate weights of deployable despun antennas. The erection and deployment technique is essentially that shown in Figure 2.22 where a central column supports the collapsed antenna during launch. Thus for a 25 ft (300 inch) diameter antenna, a weight of 25 lbs has been allocated for a supporting mast. The gain and weight curves plotted in Figure 2.13 are cross plotted onto Figure 2.15 to give the gain-weight relationship for despun 300 MHz antennas.

2.4.3.3 Antenna Weight - 3-Axis Stabilized Spacecraft

In the same manner as in the previous section, the weight variation of a deployable antenna has been calculated. Here it is assumed that the antenna deploys symmetrically from the forward equipment platform of the spacecraft. A weight allowance of 10 lbs is made for the deployment mechanism for a 300 inch aperture. Again, a cross-plot has been prepared onto Figure 2.16.

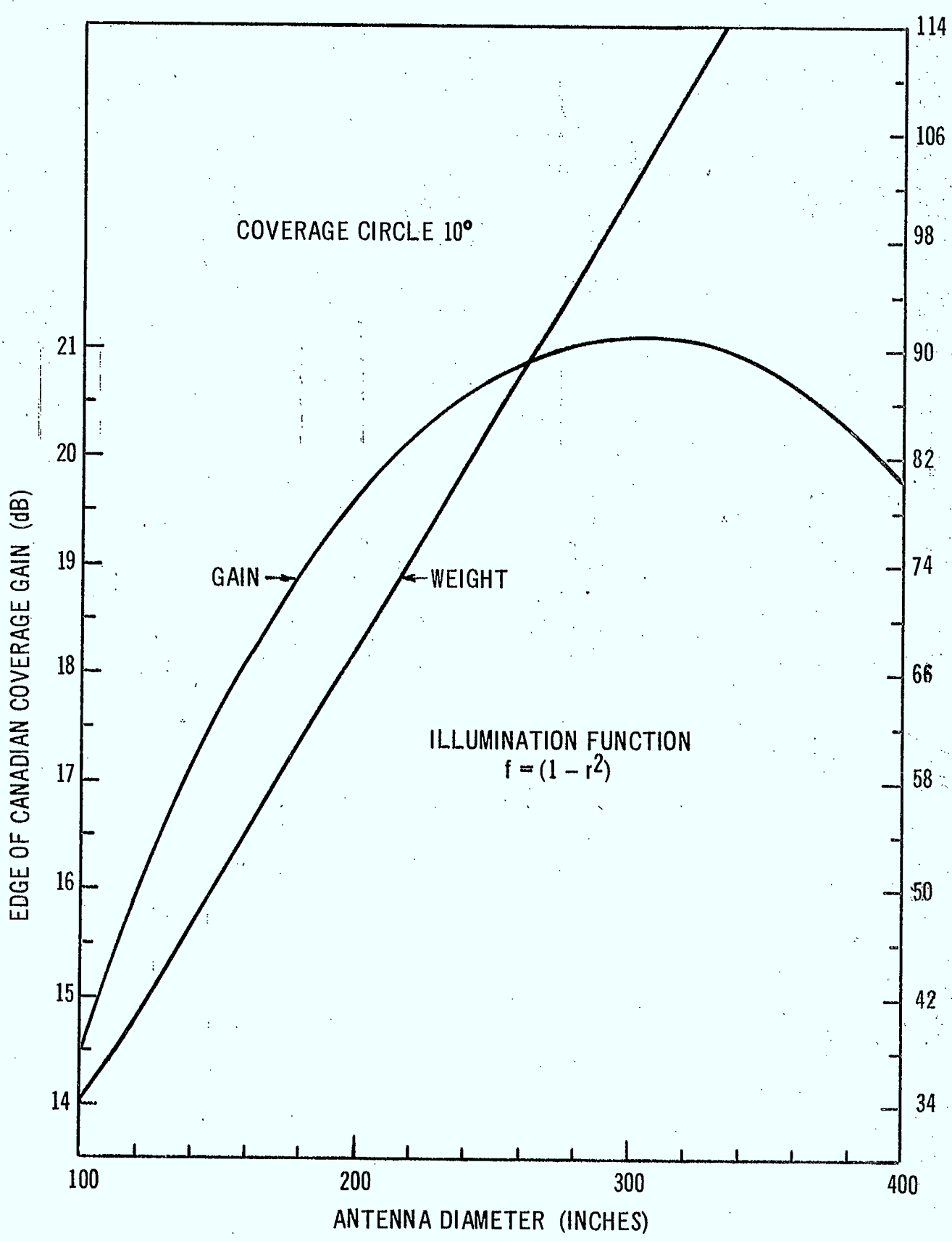

Figure 2.13 – Gain, Weight & Diameter for 300 MHz Deployable Circular Paraboloid Antennas – Spin Stabilized

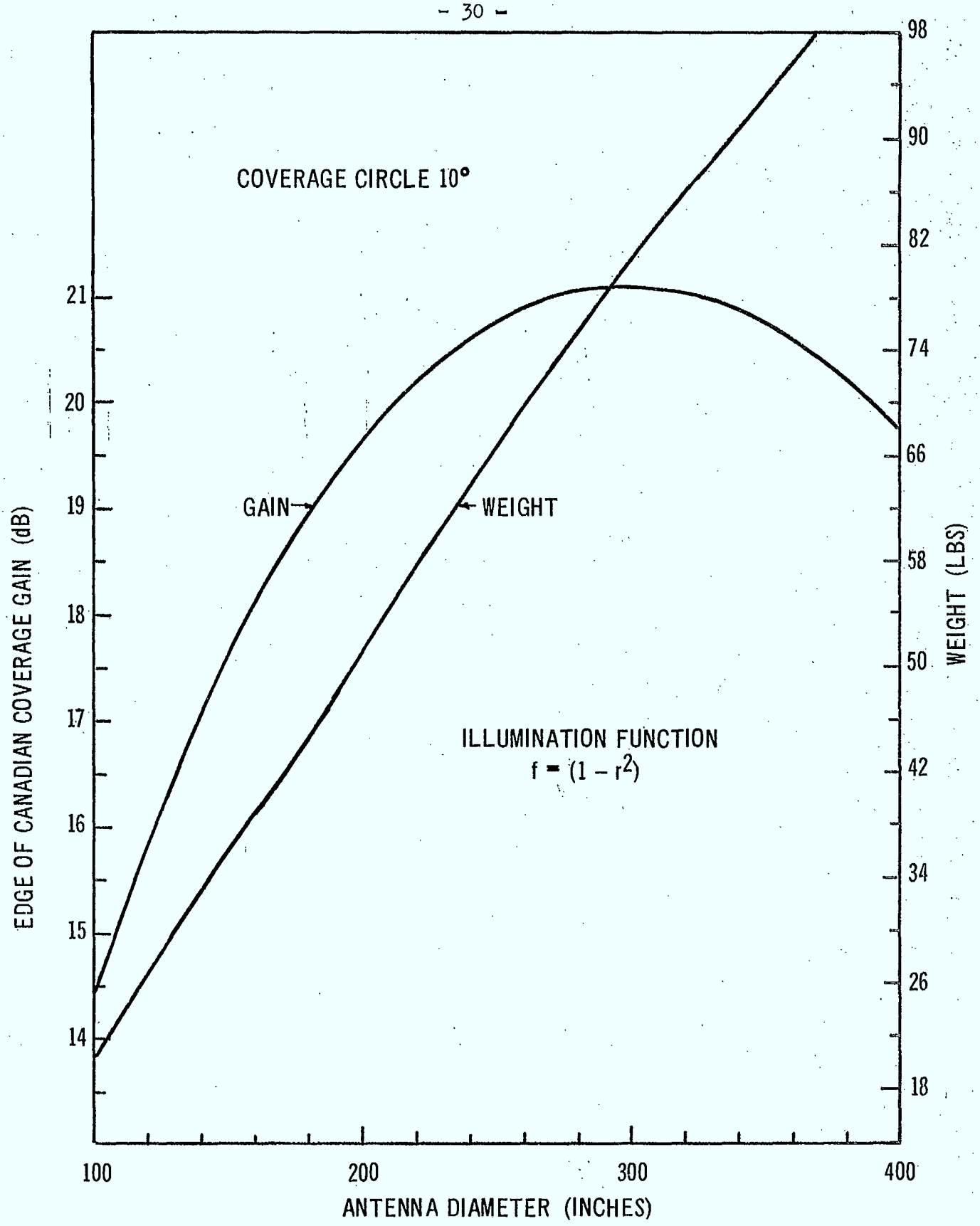

Figure 2.14 – Gain, Weight & Diameter for 300 MHz Deployable Circular Paraboloid Antennas – 3-Axis Stable

2.4.4 Choice of 300 MHz Antenna

For system reasons, the chosen 300 MHz spacecraft is a 3-axis stabilized body and hence Figure 2.15, which refers to a spin-stabilized body, is not directly applicable. However, although it is pertinent to the 1.5 GHz system described later, it will be discussed here.

(i) Figure 2.15 - Spin Stable

The most notable result of the weight analysis is that the deployable quad-helix appears to offer a better weight performance than the paraboloid for gains below 17.7 dB. The rapid decrease in paraboloid edge gain for low weight reflectors is due primarily to increased blockage effects. The curve might otherwise be expected to follow that for the quad-helix. However, for gains above 18 dB, the paraboloid is superior. This last comment is relevant to the 1.5 GHz antenna choice for a despun paraboloid.

The switched circular array, for the reasons stated in Section 2.3 is very suitable for gains below 11 dB but is unlikely to find application where high gain is required.

(ii) Figure 2.16 - 3-Axis Stable

The curves here show the same general behaviour as described above, and the choice must be for a quad-helix. However, the deployable single helix would appear to be a very good candidate provided spacecraft dynamics and antenna pointing requirements are not adversely affected by a very long helix. This is an area which could profitably be investigated. Very long helices have been measured experimentally and show suitable gain performance for the present application. For example, a 436 inch long helix at 300 MHz can provide a peak gain of 18 dB and an edge of (8°) coverage gain of 17.6 dB[9].

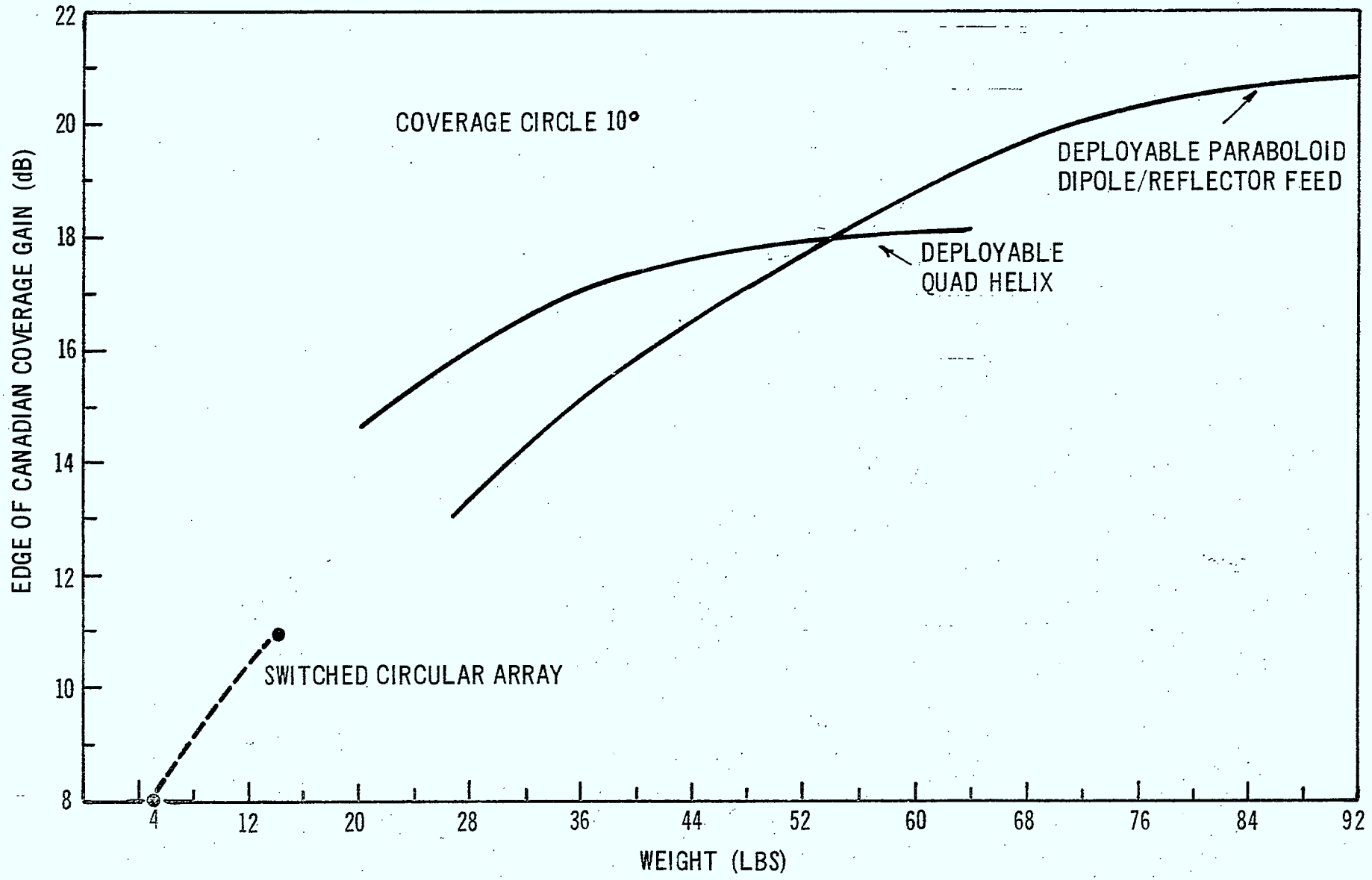

Figure 2.15 – Gain-Weight Relation for Despun Deployable Antennas – 300 MHz

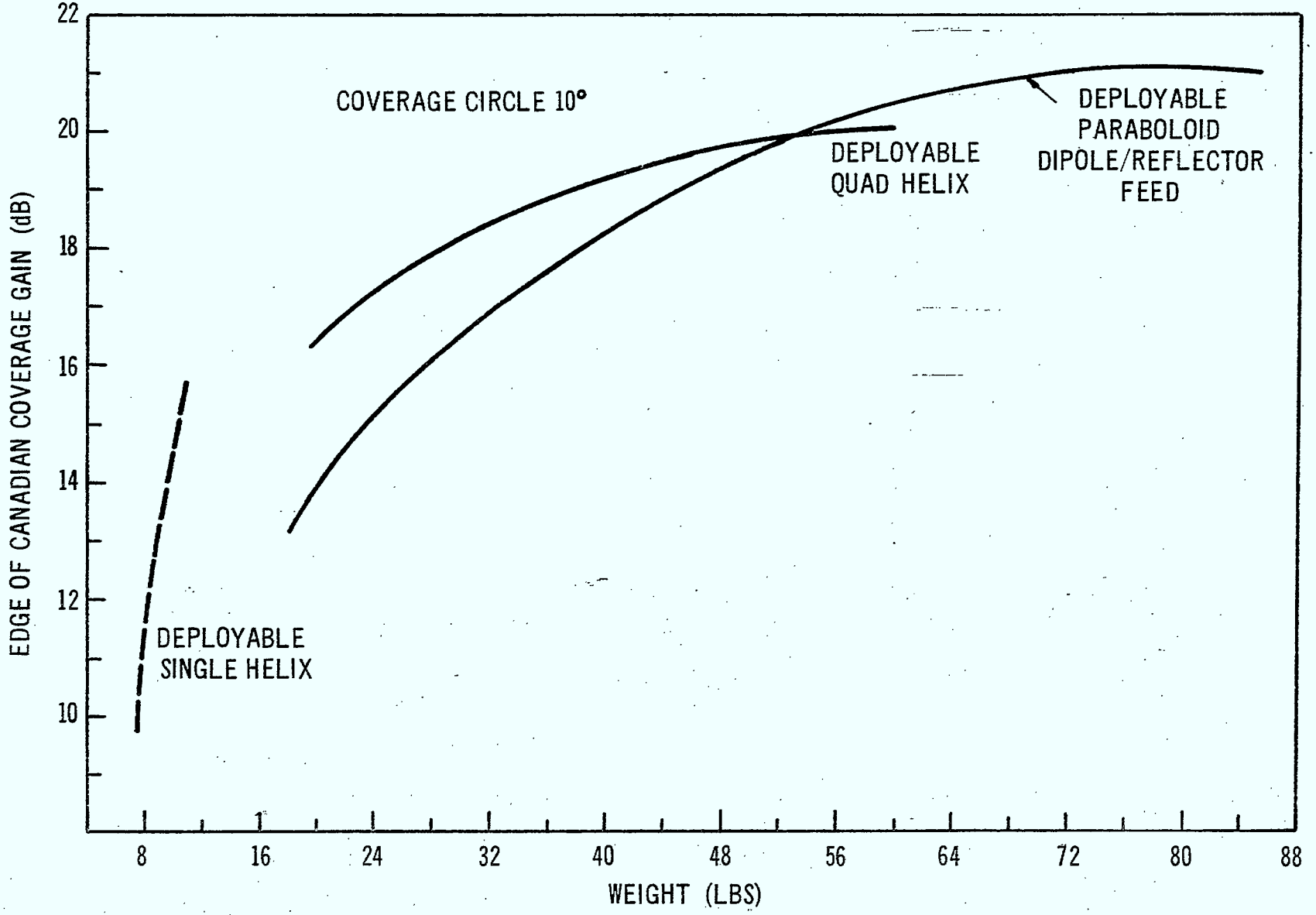

Figure 2.16 – Gain-Weight Relation for 3-Axis Stable Deployable Antennas – 300 MHz

The following characteristics of the 300 MHz antenna can now be listed in Table 2.1.

TABLE 2.1

CHARACTERISTICS OF 300 MHZ ANTENNA FOR 3-AXIS STABILIZED SPACECRAFT

Type	Deployable Quad-helix
Length of helix	95 inches
Element spacing (on side of square)	74 inches
Peak gain	19.75 dB
Edge of (8°) cover gain	18.7 dB
Ellipticity	Less than 2 dB
Weight	33 lbs.

2.4.5 1.5 GHz Deployable Paraboloids

2.4.5.1 Choice of 1.5 GHz Antenna

Following the argument of the previous sections, the optimum antenna for the spin-stabilized 1.5 GHz spacecraft is taken as a deployable paraboloid. However, the gain-weight variation for the 3-axis stabilized configuration is discussed also.

2.4.5.2 Gain

Gain at 1.5 GHz versus diameter has been calculated on the same basis as previously for $(1 - r^2)$ illuminations for different coverage circle diameters (8°, 9°, and 10°). These, as a function of diameter, are plotted in Figure 2.17. Thus, the maximum edge of (8°) cover gain of 23.8 dB is achieved with an 80 inch

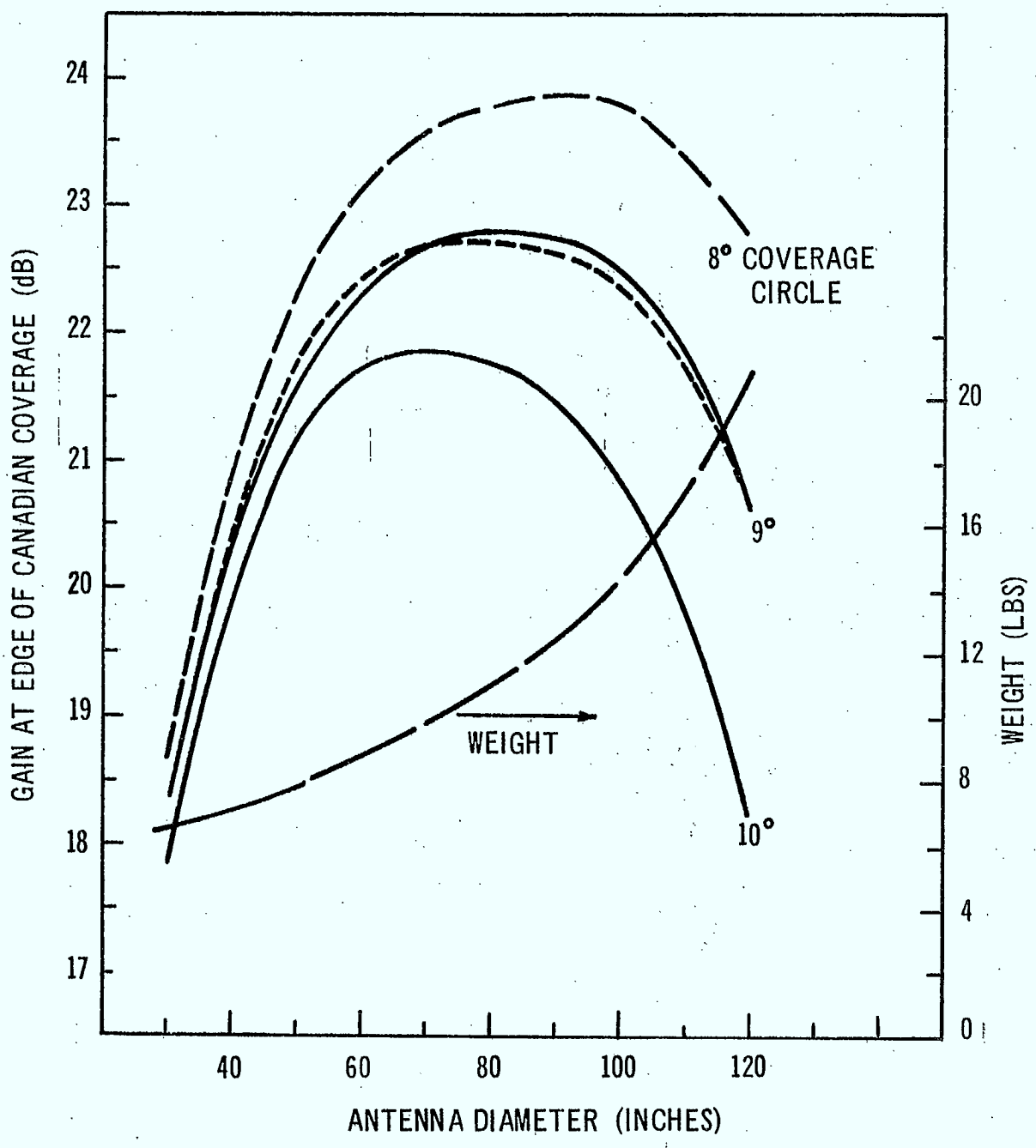

Figure 2.17 – Gain, Weight & Diameter for 1.5 GHz Deployable Circular Paraboloid Antennas – 3-Axis Stable

diameter circular aperture. Shown dotted is the edge of cover gain for a $.3 + .7(1 - r^2)$ illumination. The difference is not significant.

2.4.5.3 Weight - 3-Axis Stabilized Spacecraft

Figure 2.9 has again been used to determine the weight variation with diameter plotted also on Figure 2.17, for the 3-axis stabilized spacecraft. For example, to the basic deployable antenna weight of 8.5 lbs is added a 2.5 lb allowance for the deployment mechanism for the 80 inch aperture.

The gain-weight curve is plotted in Figure 2.19.

2.4.5.4 Weight - Spin-Stabilized Spacecraft

The gain-diameter variation for only the 8° coverage case is shown in Figure 2.18. The weight variation is essentially similar except that the weight breakdown for an 80 inch reflector with deployment mechanism as shown in Figures 2.22 and 2.23 is now as follows:

Antenna	8.5 lbs
Deployment mechanism	3.0 lbs
Support Column	8.0 lbs
Attachment collar	2.5 lbs
	22.0 lbs

2.4.5.5 Gain-Weight Relation of 1.5 GHz Paraboloids

Figures 2.17 and 2.18 are cross-plotted onto Figure 2.19 to give the gain-weight relationship for both spin-stable and 3-axis stable configurations.

The characteristics of the chosen 1.5 GHz antenna for the spin-stabilized configuration are listed in Table 2.2.

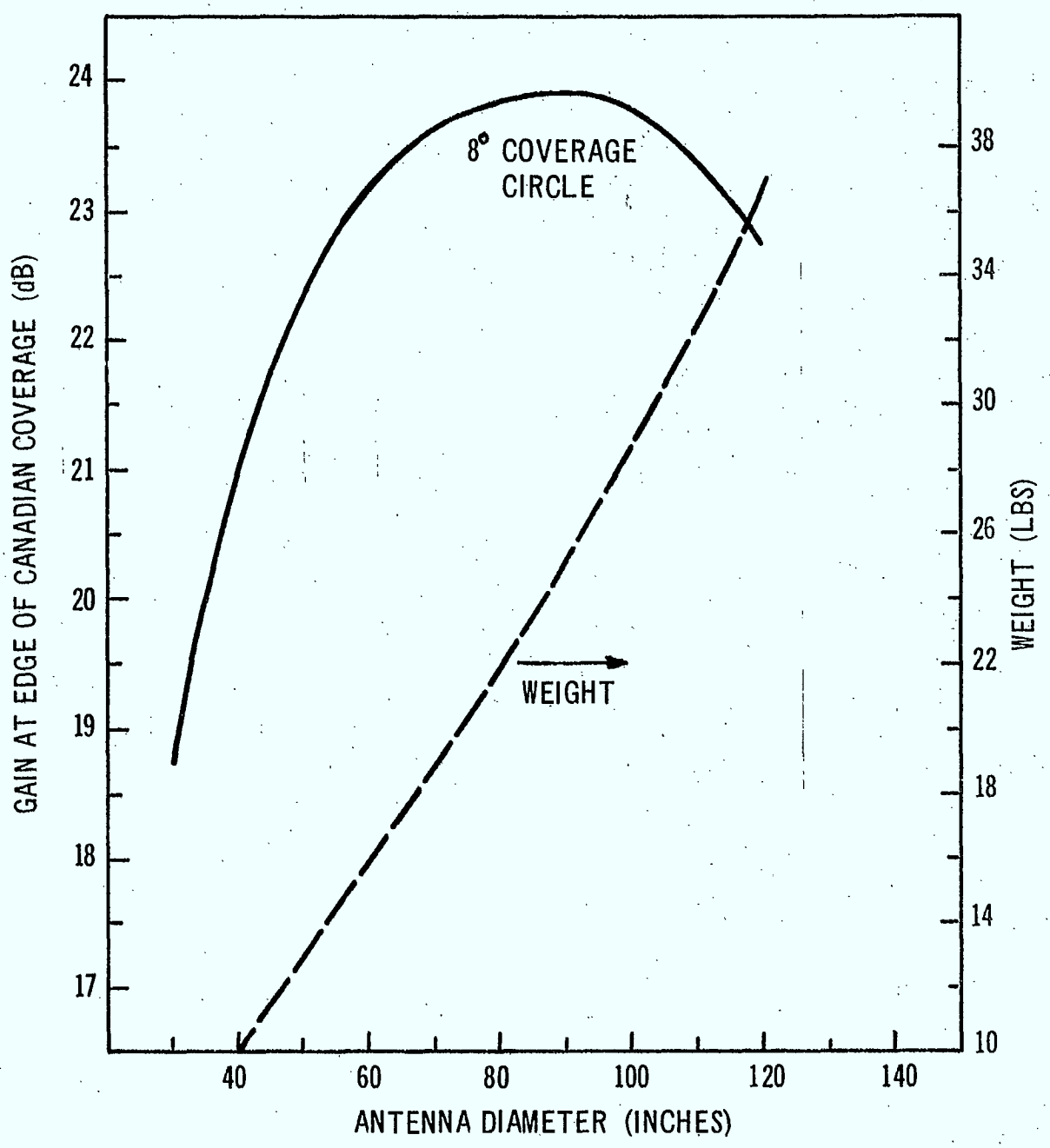

Figure 2.18 – Gain, Weight & Diameter for 1.5 GHz Deployable Circular Paraboloid Antennas – Spin Stable

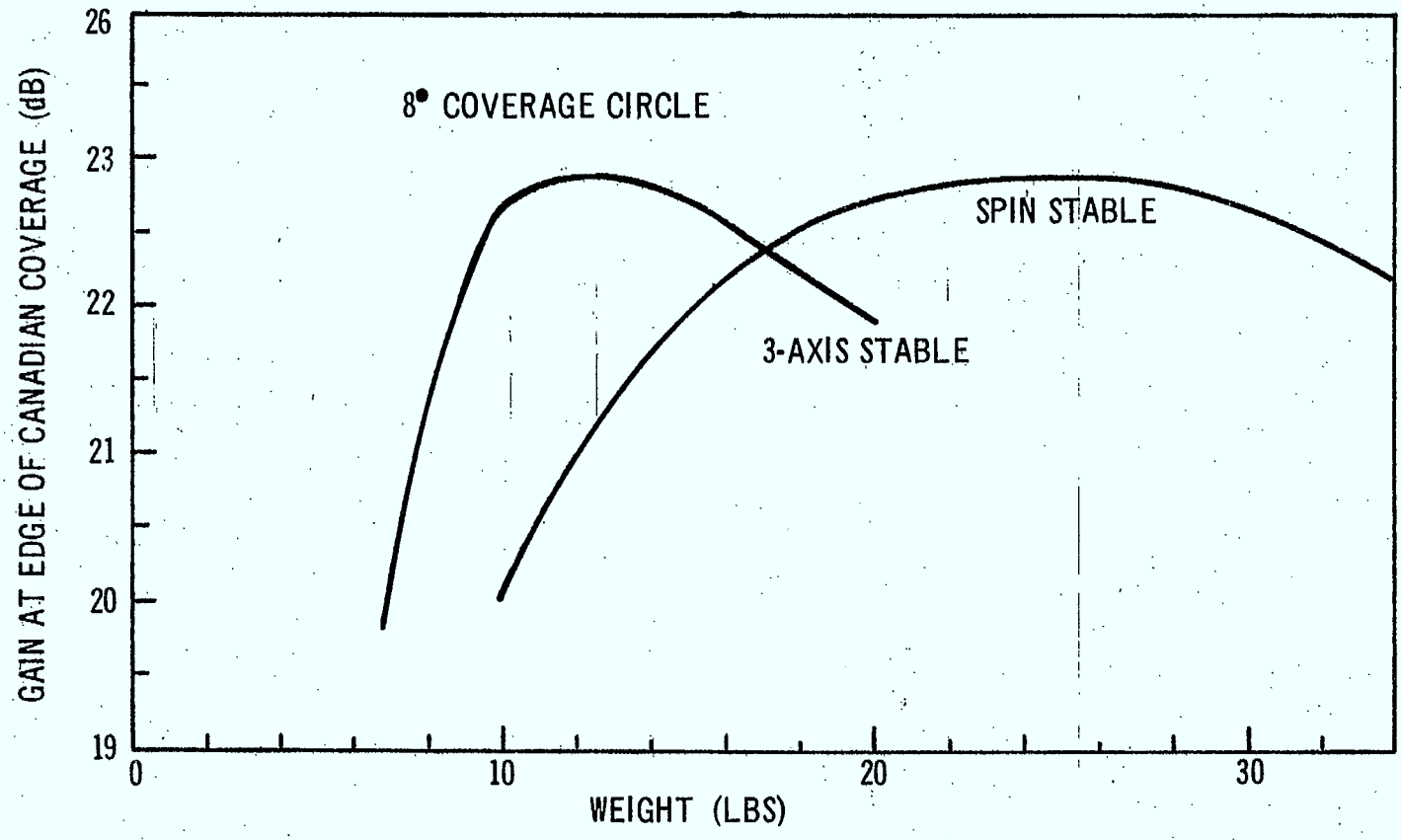

Figure 2.19 – Gain-Weight Relation for Deployable Circular Paraboloids

TABLE 2.2

CHARACTERISTICS OF 1.5 GHz ANTENNA FOR SPIN-STABILIZED SPACECRAFTS

Type	Deployable Paraboloid
Diameter	80 inches
Peak gain	27.3 dB
Edge of (8^{o}) cover gain	23.8 dB
Ellipticity	Less than 2 dB
Weight	22 lbs.

2.5 Proposed Antenna for the 1.5 GHz Spacecraft

2.5.1 Electrical Design

(a) Feed

A suitable feed element has been described by Svennerus[10]. This is a circularly polarized two-turn helix with a central supporting column, electrically decoupled from the helix. A conical ground plane or shield gives low spillover losses. The E_θ and E_ϕ principal plane radiation patterns are shown in Figure 2.20, taken from Ref. (10). The slight difference in edge taper is not sufficient to cause a noticeable change in ellipticity or coverage.

The approximate electrical dimensions are also indicated so that the blocking diameter would be approximately 6 inches, low enough for satisfactory performance. The central column is approximately 0.8 inches diameter.

(b) Reflector

The feed patterns are suitable for a reflector with an F/D ratio of around 0.37 which is a satisfactory value for efficient illumination. Thus,

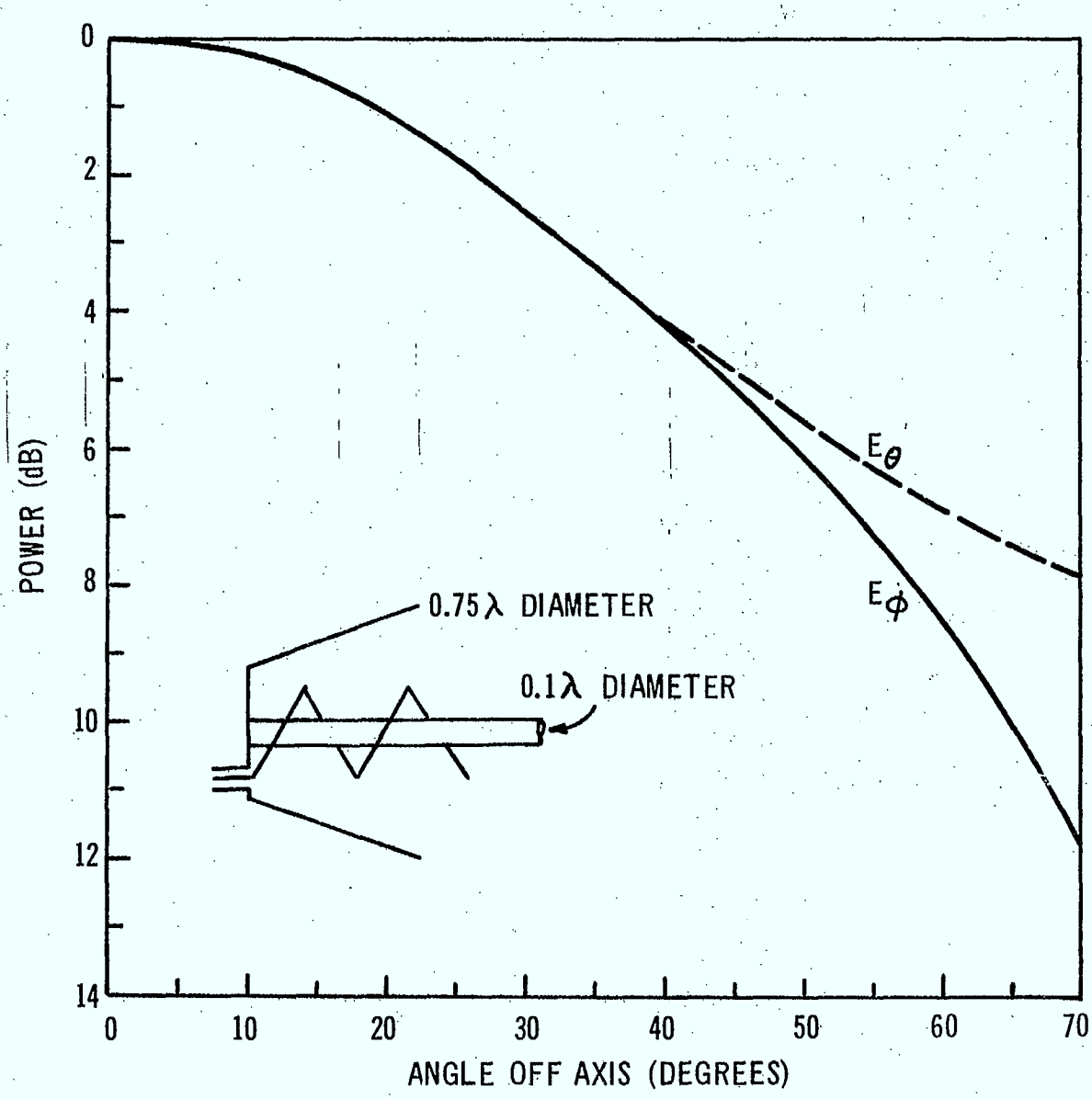

Figure 2.20 – Radiation Patterns of Two-Turn Helix with Conical Shield

the focal length is approximately 29.6 inches. The secondary radiation patterns for two different edge tapers with parabolic illumination are shown in Figure 2.21.

2.5.2 Mechanical Design

(a) Reflector

The reflector is an umbrella-folding surface with aluminum radial ribs of U-channel cross-section approximately 1 inch deep. The ribs are preformed to give a best fit surface when deployed. The reflecting surface is gold-plated nichrome mesh with a mesh hole diameter of less than .1 inch. A stainless steel tensioning wire around the perimeter allows fine adjustment to the reflecting surface focussing.

When folded, the reflector occupies a volume approximately 40 inches × 10 inches diameter.

(b) Deployment Mechanism

The deployment technique is illustrated in Figures 2.22 and 2.23. There are three distinct phases:

(i) Spacecraft Spin-up

The antenna rib-tips, in the collapsed position, are locked to the top deck as is the antenna support tube through the despin motor.

(ii) Antenna Erection

Just prior to antenna despin, the rib-tips locking collar is removed and, under the combined effect of centrifugal force and a spring-loaded hinge, the antenna, still collapsed, is erected to its on-axis position.

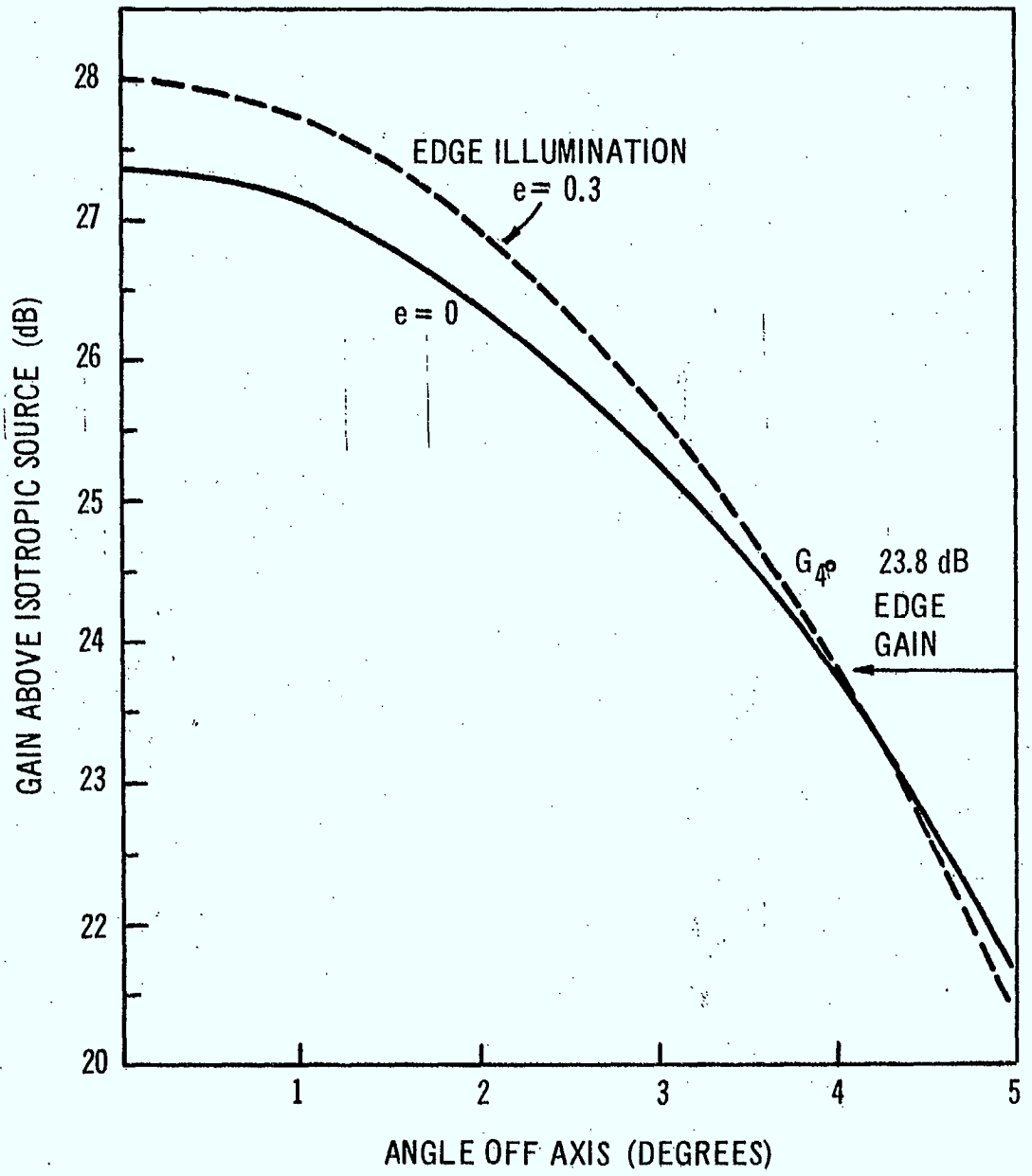

Figure 2.21 – Radiation Patterns of 80-inch Diameter Circular Paraboloid

(iii) Antenna Deployment

As the antenna reaches its on-axis position, spring loaded latches engage the antenna back-plate. The antenna momentum compresses a spring-loaded end-stop, allowing the drive spring release actuator to release the deployment drive spring. The drive spring then deploys the antenna fully, pushing the hinged rib ends against end stops.

The feeder cable is allowed to warp as it is pushed into the support tube.

2.5.3 Thermal Design

Since the antenna reflector is of mesh construction, thermal distortion will be kept to a minimum. It is estimated that a 1" diameter feed tube will have a peak tip deflection of 0.03 inches in the thermal environment. At a 29.6 inch focal length, this will cause a thermal pointing error of .05 degree.

The reflector ribs will experience a similar bending which may cause a peak pointing error of .1 degree.

The antenna support tube will cause only pointing errors in roll or yaw. Roll errors (i.e. N-S pointing errors) are of no importance for oversize radiation patterns, whilst yaw errors, especially for circular, circularly polarized beams, are of less significance.

It is expected then that the maximum pointing error will not exceed .15 degrees.

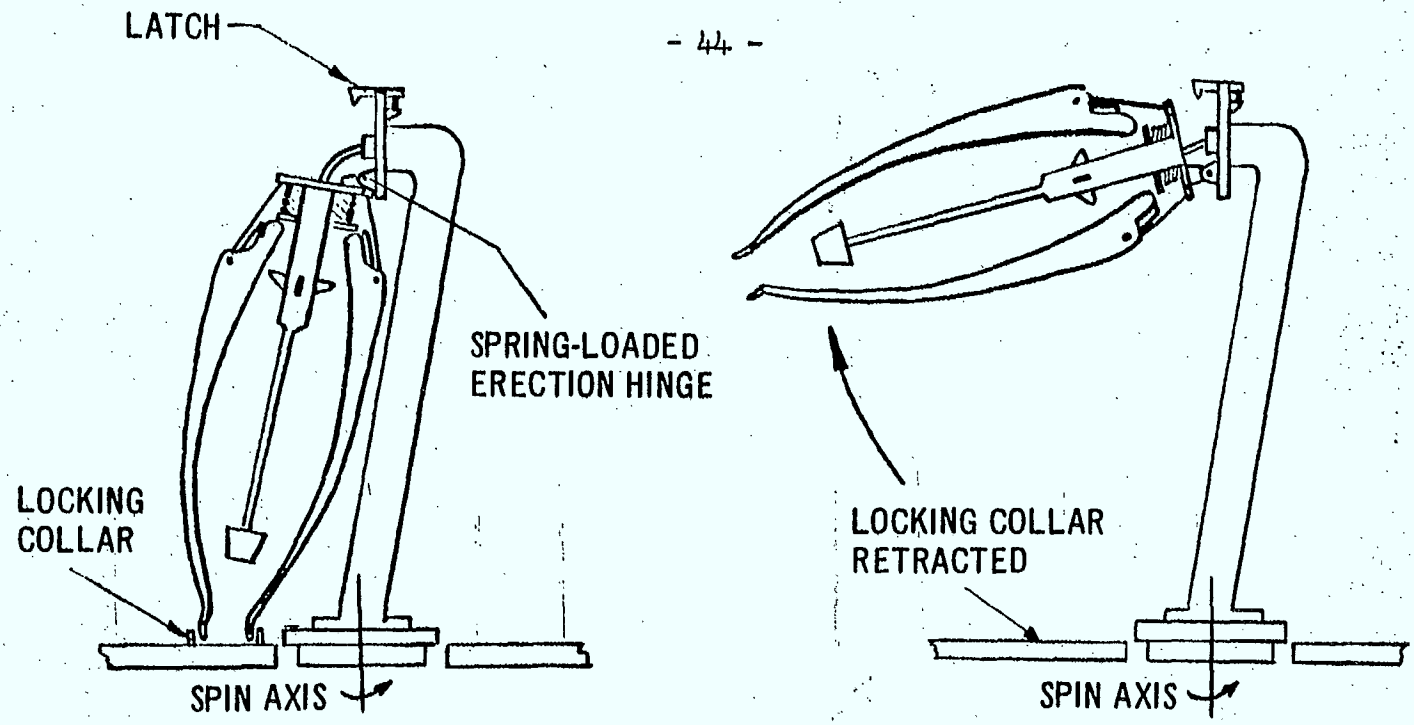

(1) Spacecraft Spin-up Configuration

(2) Antenna Erection

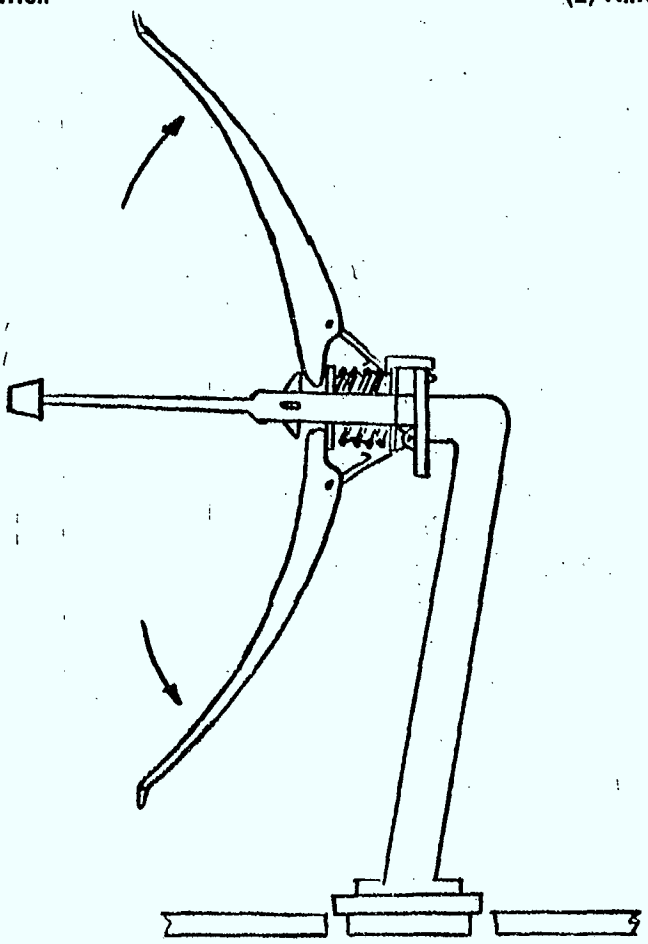

(3) Antenna Deployment – Despun Antenna

Figure 2.22 – 1.5 GHz Deployable Antenna Concept

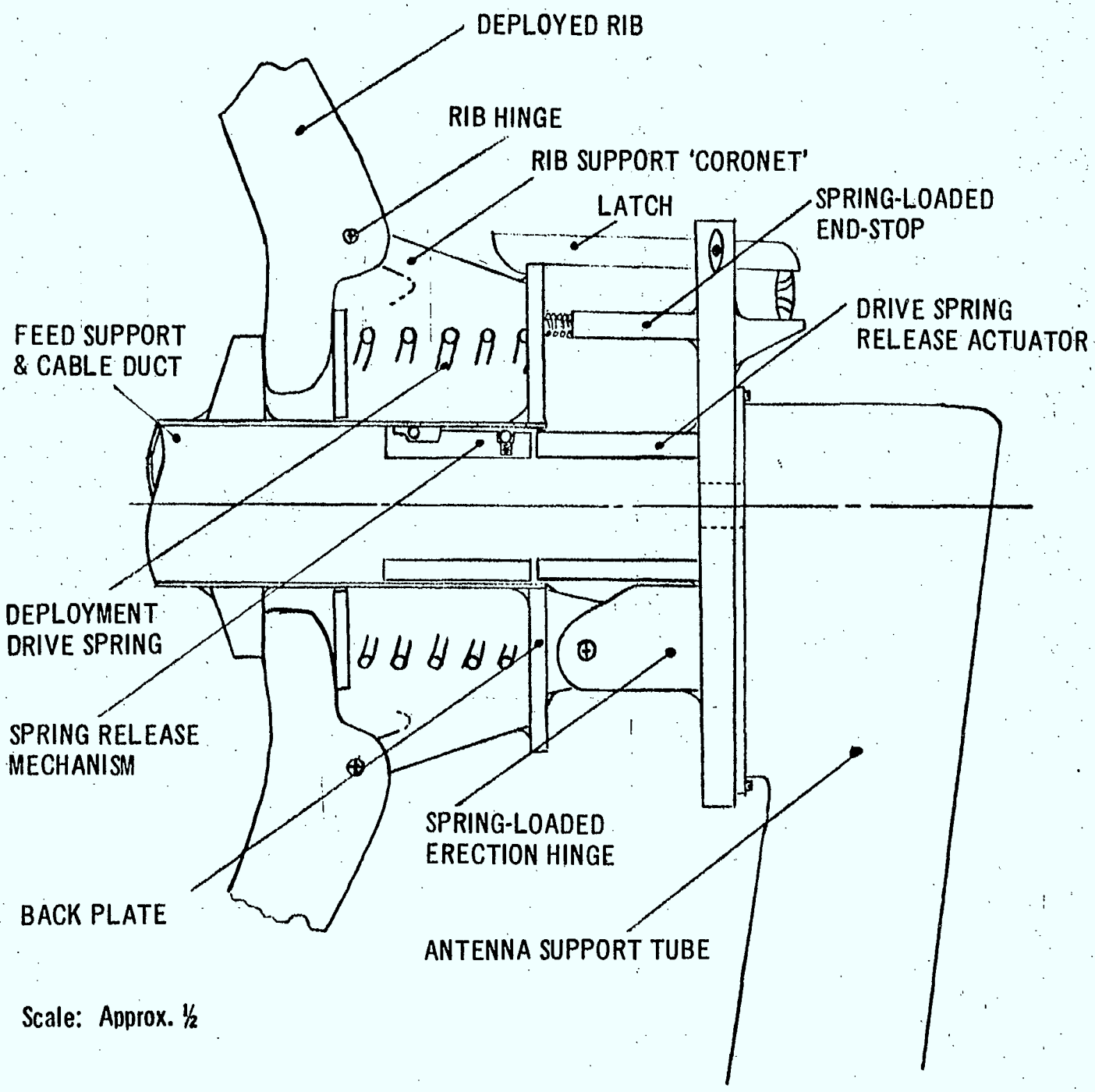

Figure 2.23 – 1.5 GHz Deployable Antenna Mechanism

2.6 References

1. W. Rebhan, "Radiation Patterns of Communications Satellite Aerials", Frequenz, Vol. 20, No. 5, May 1966.

2. R. Holland, "Optimization Criterion for Illuminating Circular Antenna Apertures", IEEE Trans. Antennas and Propagation, May 1971.

3. K. Milne and A.R. Raab, "Optimum Illumination Tapers for Four-horn and Five-horn Monopulse Aerial Systems", Conf. on Design & Construction of Large Steerable Aerials, IEEE Conf. Publication No. 23, May 1966.

4. J.D. Kraus, "Antennas", Chap. 7, McGraw-Hill, New York 1950.

5. "Hughes Multipurpose Synchronous Communications Satellite Study", Final Report, Vol. 1, August 1967: Communications Satellite Corp. Contract Number CSC-SA-8.

6. D.C. MacLellan, H.A. MacDonald, P. Waldron, H. Sherman, "Lincoln Experimental Satellites 5 and 6", AIAA Paper No. 70-494. AIAA 3rd Communications Satellite Systems Conference, Los Angeles, April 1970.

7. J.D. Kiesling and W.S. Maco, "An Electronically Despun, Switched Antenna", AIAA Communications Satellite Systems Conference, Washington, May 1966.

8. S.A. Milliken, "The Development of High Gain Deployable Antennas for Communications Satellites", AIAA Paper No. 66-306. AIAA Communications Satellite Systems Conference, Washington, May 1966.

9. T.S.M. Maclean, "Measurements on High-gain Helical Aerials and on Helical Aerials of Triangular Section", Proc. IEE, Vol. III, No. 7, July 1964.

10. G. Svennerus, "Some Aspects of the Design and Use of the Helical Antenna", Proc. of the International Congress, UHF Circuits & Antennas, Paris, October 1957.

3. TRANSPONDER SUBSYSTEM

3.1 Types of Transponder

3.1.1 General

There are a number of possible transponder configurations that might meet the requirements of the thin route traffic system. These are listed in Table 3.1 along with the characteristics of each. Early in the program these configurations were given a very cursory examination and two (Nos. 2 and 3) were selected for more detailed study. The reasons why the others were discarded are discussed below. Table 3.1 gives a rating on complexity, indicates if intermod is present, if back-off of the output amplifier is required and indicates whether companding, voice activation and pre-emphasis are possible. An entry of "yes" in these three columns means that the technique is not only possible but that there is an advantage to the satellite to do so. An entry of "no" means that either the technique is not possible or that no advantage to the satellite results.

The first transponder configuration is a fully channelized version. Each of the 200 audio channels and 5 radio channels has a separate power amplifier operating at 1.5 GHz. These channels are then multiplexed together in a 205 channel multiplexer for radiation from the antenna. This is a very complex configuration and has a very difficult multiplexer design problem. This configuration was not considered further.

The second system is a single channel transponder. This is a very simple system as no signal processing takes place on board. There is only a single frequency shift from the input to the output. Thus all the audio channels pass through the power amplifier on separate carriers which must be

	Complexity	Intermod	Back-off Required	Voice Activation Possible	Pre-emphasis possible	Companding possible	Comments
1. Fully Channelized	very high	none	no	yes	Yes	yes	Multiplexing is difficult
2. Single Channel	low	yes	yes	yes	yes	yes	
3. Three Channel	moderate	yes	yes	yes	yes	yes	
4. Single Carrier (base band)	very high	none	no	yes	yes	yes	
5. Single Carrier (double modulation)	moderate	none	no	yes	yes	yes	Low FM improvement obtained

TABLE 3.1 - Comparison of Different Transponder Configurations

backed off to a linear region to reduoe intermod. This reduoes the efficiency of the power amplifiers but advantage can be taken of improvement due to oompanding, voice activation and pre-emphasis. It is considered a viable system and has been developed in more detail.

The third system is a variation of the second. There are three types of service required. The radio channels have a high carrier level and produce high level intermod in the region of the low level carriers. Thus the low level carriers must be raised aocordingly. By separating the three servioes into three separate channels this penalty can be avoided. This also was considered a viable system and has been examined in some detail.

The fourth system utilizes a single carrier on the down link so that no intermod is generated and the output power amplifier oan be driven into saturation for high efficiency. The single carrier is obtained by completely demodulating the audio ohannels down to baseband and then stacking them up for final modulation on a single carrier. This system suffers from a high complexity in the demodulation and modulation circuitry on the satellite. It was not considered further.

The fifth system also gives a single oarrier on the down link resulting in high efficiency for the output power amplifier. It is also possible with this system to obtain improvements due to companding, voice activation and pre-emphasis. It has a problem with bandwidth however. Because the uplink signal is not demodulated on the satellite the bandwidth of the signal modulating the downlink oarrier is wider than the total audio baseband. There are two possibilities. One is to use a lower modulation index and the second is to use a higher downlink bandwidth. In the first case the required FM improvement

factors are not obtained and in the second case the thermal noise is increased resulting in higher required transmitter power. This configuration was not fully evaluated but tentative calculations indicated that, compared to configuration No. 2, the advantage due to saturated operation on the downlink was more than lost by the increased power required to overcome the increased thermal noise. Because it was not evident that the extra bandwidth was available this system was not considered further.

3.1.2 Single Channel

This transponder (item 2 in Table 3.1) is a single translation type with no signal processing on board. The signal in the uplink band is received on the antenna. It first passes through a duplexer or circulator to isolate the receiver from the transmitter. A filter is included in the receive line to provide additional isolation from the transmitter. After the input filter is a low noise amplifier followed by a frequency down converter from uplink to the downlink band. A second filter removes the uplink band. The transmitter frequency band is then amplified by an amplifier and driver combination to sufficient power level to drive the output power amplifier. The multiple device power amplifier is driven by a dividing network (described later) so that every device is driven at the same level. A similar network combines the output signals. The final element in the transponder is a third filter which removes noise in the receive band that may have been generated in the power amplifier. The block diagram of this transponder is shown in Figure 3.1.

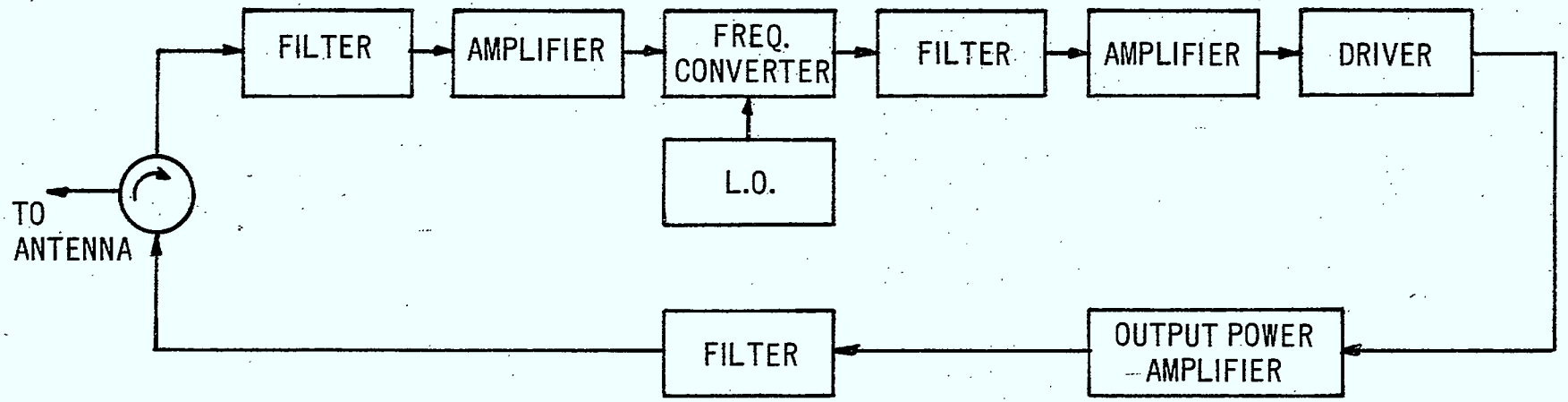

Figure 3.1 – Single Channel Transponder Configuration

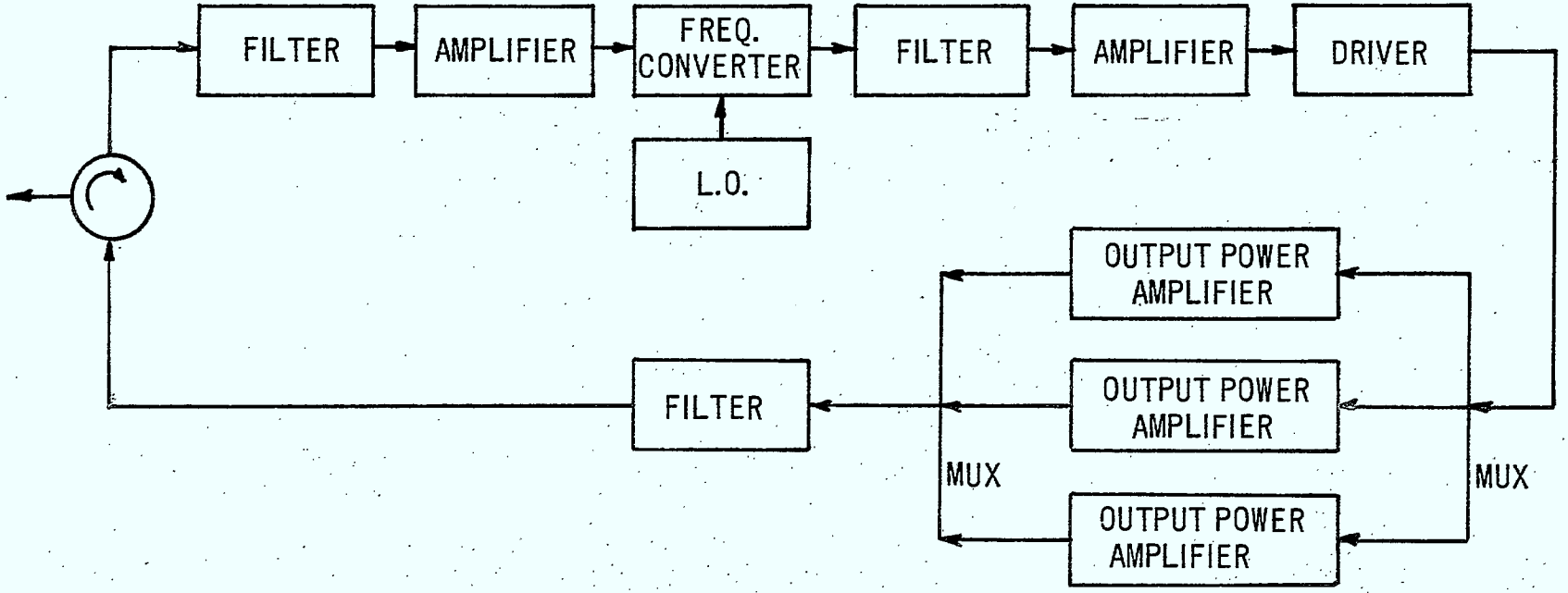

Figure 3.2 – A Three Channel Transponder Configuration

3.1.3 Channelized Transponder

A transponder with three output amplifiers has also been considered (Figure 3.2). This has one amplifier for the commercial channels, one amplifier for the private channels and one amplifier for the radio program channels. An input and output multiplexer are added to feed the three frequency bands to their respective amplifiers and to combine the output signals into a single transmission line. The rest of the transponder is essentially the same as for the single amplifier transponder.

It was hoped that by separating the traffic into three separate amplifiers each of narrower bandwidth a net reduction of intermod level would result. However, sufficiently accurate knowledge of intermod levels in transistor amplifiers has not been available for this to be accomplished and only the single amplifier transponder will be considered further.

3.2 Power Amplifier Devices

3.2.1 Vacuum Devices

There are three types of devices that have been considered for the output power amplifier of the transponder. These are travelling wave tubes (TWT), transistors and beam power triodes or tetrodes. For the higher frequency (1.5 GHz) transistors and TWTs have been considered and for the lower frequency (400 MHz) the choice has been between transistors and beam power tubes.

Travelling wave tubes are generally used as power output devices for satellite transponders. For this reason a fund of design information has been built up about TWTs in this application. However, no TWT currently exists

for the power level and frequency required for the current application. Thus a travelling wave tube to fulfill the requirement would have to be especially developed.

In the case of beam power tubes there is no fund of knowledge for a transponder application in space. The usual application for 400 MHz tubes of this type is in ground based oscillators and amplifiers. They are usually replaced after about one year of operation in the course of regular maintainance. To increase the reliability of these tubes they would have to be greatly derated. In addition existing tubes are cooled by forced air. However, at least one tube is available with BeO conduction cooling (RCA type 8828). Some considerations of a transponder using this tube will be discussed below. Data on a number of representative tube types is given in Table 3.2.

3.2.2 Solid State Devices

Transistors for use in the power output amplifier have the advantage of being solid state having no heater power requirements with the subsequent burn out life of the cathode. They also have the advantage of the high reliability of solid state devices.

Power transistors are presently available at frequencies up to 2.5 to 3.0 GHz with reasonable output power levels and efficiencies. In addition, this is an area of rapidly developing technology and one can expect further advances in the next few years. For single carrier operation the transistors can be operated Class C at high efficiency. However, the present application calls for multicarrier operation where intermod results due to interaction between the carriers in the nonlinear impedances of the junction.

Tube Type	Weight ounces	Frequency MHz	Power Class AB	Cooling
8121	3	400	100W	fin
8122	3.5	400	200W	fin
8072	2	400	100W	conduction
8828	4	400	200W	BeO block
7650	12	400	600W	
8226	4	400	150W	

TABLE 3.2 - Performance Parameters of 400 MHz beam power tubes.

This is of major concern and one that is treated in more detail in the section on intermod.

A list of representative transistors with major operating parameters is given in Table 3.3.

3.3 Intermodulation Considerations

3.3.1 System Consideration

The intermodulation levels produced in the output amplifier are of concern in the system design considerations. The intermod levels assumed in the system calculation are lower than the downlink thermal noise contribution but are at such a level that any increase in intermod will increase the EIRP required to meet the system performance specification. The level assumed for the multicarrier intermod level was -16.5 dB. This translates to about -24 or -25 dB for a two tone test situation. Two approaches have been investigated. A push pull amplifier was investigated for intermod cancellation. It is shown that this was not possible under conditions where the fundamental signals were added. A transistor amplifier at 1.8 GHz has been laboratory tested for intermod and conditions found which would give low intermod at high efficiency.

3.3.2 Intermod Levels in Class C Transistor Amplifiers

A number of workers have investigated third order intermod in transistor amplifiers. Some of these have demonstrated low intermod without being too specific about how it was obtained. Others have worked at much lower frequencies than those considered here.

Manufacturer	Type No.	GHz Freq.	Class	θ_{J-C} °C/W	Power Watts	dB Gain	Eff.	Comments
RCA	7994	1.5	A	-	2.0	>10	~30%	
RCA	7994	1.5	C	8.5	10	10	45%	
RCA	7995	1.5	A	-	2.5-3	>10	~30%	
RCA	7995	1.5	C	-	15	10	45%	
RCA	8174	1.5	A	-	5	10	~30%	Projected early 1972
RCA	8174	1.5	C	-	23	10	45%	Projected early 1972
RCA	7706	.4	C	3.5	30	5	80%	
MSC	MSC3005	2.5	C	-	6	7	35%	

TABLE 3.3 - Performance Parameters of Existing or Projected Transistors

Hilling and Salmon[1] have shown that third order products are related to gain flatness for changes in emitter current. Operating in the 50 to 500 MHz band they obtained best performance of 25 to 30 dB intermod level at emitter currents giving maximum gain flatness.

Chang and Locke[2] show low intermod operation of a class C transistor operating at 30 MHz. They obtain low intermod between the two limits of linear operation, i.e. at high power where saturation occurs and at low power with insufficient forward bias. They obtained an intermod level lower than 30 dB over a 10 dB dynamic range. No special operating conditions were specified to obtain this performance at 30 MHz.

Thomas[3] has carried out both experimental and theoretical work on intermod. He shows analytically that the intermod produced by one nonlinearity in the transistor may be cancelled by that produced by another nonlinearity since these products are inherently 180° out of phase. Experimental measurements confirmed these findings.

Boag and Newby[4] have measured intermod levels in a single 2N5470 coaxial transistor class C amplifier operated at 1.8 GHz. When adjusted for maximum power output the intermod level ranged in general between -10 and -15 dB. Some measurements, however, gave intermod levels of -26 dB at high drive level and high efficiency.

Two tone intermodulation level measurements have been repeated using the setup of Boag and Newby. These measurements were specifically aimed at demonstrating that low intermod and high efficiency could be obtained simultaneously with Class C operation. An additional objective was

to determine the dynamic range over which low intermod was maintained. By detuning the input and output of the transistor and adding a small amount of bias the amplifier could be adjusted for intermod levels that ranged between 25 and 30 dB below the level of the two carriers. This was accomplished at a slight loss in efficiency of about 0.6 dB. This loss in efficiency has reduced the specified Class C efficiency of 80% at 400 MHz to 70%. Currently quoted Class C efficiencies are 45% at 1.5 GHz and 35% at 2.5 GHz, and these reduce to 39% and 30% respectively for low intermod operation.

Some measured results considered typical of the type of operation considered are shown in Figure 3.3. Here the intermod level, efficiency and gain are plotted as a function of the input drive level. Over a four dB range, from 52 mw to 135 mw input power, the measurements were accomplished without readjustment other than varying the input drive level. For one final point, at 200 mw drive level, some readjustment was necessary to obtain the drive power. It is considered however that this point is one of the family indicating a total dynamic range of very nearly 6 dB where the intermod is below the required maximum of -24 dB.

3.3.3 Evaluation of Push-pull Amplifiers for Intermod Suppression

Push-pull amplifiers have been analyzed by Lambert[5] for second harmonic cancellation. He showed that if the two amplifiers in push-pull are

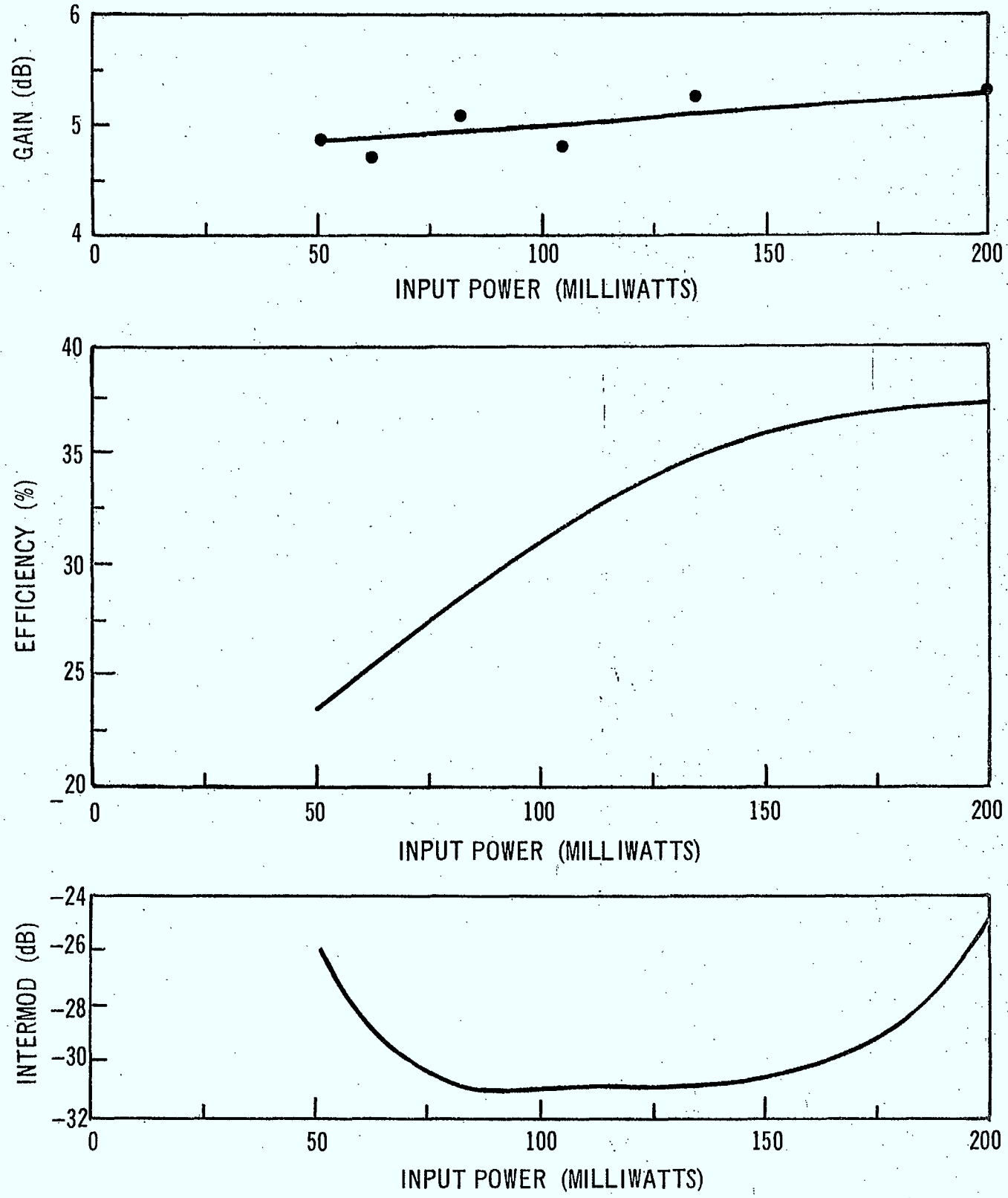

Figure 3.3 – Measured Intermod Level versus Input Power

fed in phase opposition the second harmonic components cancel. He showed that a reduction of 20 dB could be realized provided that second harmonic components were within 1.5 dB in amplitude and 5 deg. in phase.

For a narrow band amplifier however, the second harmonic is of little concern since it is removed by subsequent filtering. Instead the third order intermod components are important since they occur within the pass band of the amplifier. The following is an attempt to use a push-pull amplifier to cancel out intermod products while adding the desired fundamental components from the amplifiers. It is shown instead that this is not possible as the intermod products appear with the same phase and in the same frequency band as the desired signals. It is shown however that it is possible to cancel the third harmonic components while at the same time retaining the desired signals by driving the amplifiers in phase quadrature. This is not the same condition for second harmonic cancellation so that the second and third harmonic can not be cancelled simultaneously.

Intermod products only exist when two or more frequencies pass simultaneously through the amplifier. They occur at frequencies $2f_1 - f_2$, $2f_2 - f_1$, $f_1 + f_2 - f_3$, etc. Only the two frequency case is considered here. After Lambert, a single amplifier has an output characteristic

$$V_o = a_1 v_{in} + a_2 v_{in}^2 + a_3 v_{in}^3$$

These amplifiers are combined in a push pull amplifier shown in Figure 3.4, where ϕ is the input phase shift and θ is the output phase shift.

The input voltage is composed of two frequency components

$$v_{in} = b_1 \cos \omega_1 t + b_2 \cos \omega_2 t$$

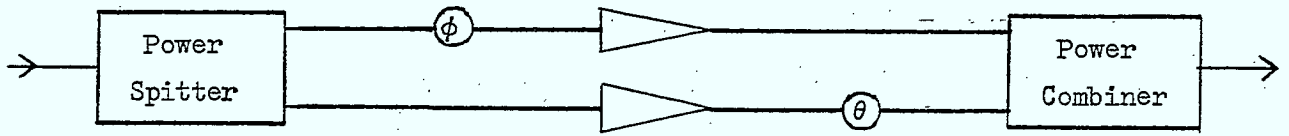

Figure 3.4 - Schematic representation of a push-pull amplifier.

The output from the push-pull amplifier is

$$V_{out} = v_{01} + v_{o2} + v_{o3}$$

where v_{o1} is the desired component and v_{o3} contains the third order distortion products. Using Lambert's notation

$$v_{o1} = .5\, a_1 x[b_1\cos(\omega_1 t + \phi) + b_2\cos(\omega_2 t + \phi)] + .5\, a_1 y[b_1\cos(\omega_1 t + \theta) + b_2\cos(\omega_2 t + \theta)]$$

$$v_{o3} = .25\, a_3 x[b_1\cos(\omega_1 t + \phi) + b_2\cos(\omega_2 t + \phi)]^3 + .25\, a_3 y[b_1\cos\omega_1 t + b_2\cos\omega_2 t]^3 e^{j\theta}$$

By expanding the above and omitting all but intermod terms v_{o3} becomes

$$v_{o3} = -\frac{3}{16} b_1 b_2\, a_3 x[b_1\cos((2\omega_1 - \omega_2)t + \phi) + b_2\cos((2\omega_2 - \omega_1)t + \phi)] - \frac{3}{16} b_1 b_2\, a_3 y[b_1\cos((2\omega_1 - \omega_2)t + \theta) + b_2\cos((2\omega_2 - \omega_1)t + \theta)]$$

Thus the intermod products have the same phase as the desired signal v_{o1} and cannot be cancelled at the same time that the desired signals are added in the output combiner.

If only the third harmonic components are retained then v_{o3} becomes

$$v_{o3} = \frac{1}{16} a_3 x[b_1^3\cos(3\omega_1 t + 3\phi) + b_2^3\cos(3\omega_2 t + 3\phi)] + \frac{1}{16} a_3 y[b_1^3\cos(3\omega_1 t + \theta) + b_2^3\cos(3\omega_2 t + \theta)]$$

The phases of the third harmonic component are not the same as the fundamental and it is possible to cancel the third harmonic while retaining the fundamental. The two conditions for accomplishing this are

$$\phi - \theta = 0 \text{ (addition of fundamental)}$$

$$3\phi - \theta = 180^\circ \text{ (cancellation of third harmonic)}$$

The solution of these two equations gives both ϕ and θ equal to 90 degrees. This could be implemented by means of ninety degree hybrids at both input and output without any additional components. This configuration would cancel the third harmonic components but retain the second harmonic since the second harmonic requires 180 degree phase shifts at both the input and output in order to give cancellation.

3.4 Power Combiners

3.4.1 Introduction

Two combining networks have been considered, a straight hybrid combiner and a star combining configuration (Refs. 6,7). The hybrid combining network is straightforward since it uses nothing but standard hybrid junctions. It has the disadvantage that the loss of one amplifier of a pair causes a drop in output of 6 dB rather than the expected 3 dB.

The star is not a developed system but promises to have some advantages in performance and reliability over a hybrid combiner.

3.4.2 Hybrid Combiners

A typical hybrid combiner is shown in Figure 3.5. This is the network proposed for the CTS UHF transponder. It uses eight transistors which are first combined in hybrids to make 4 lines. These are passed through isolators and then fed to a four way combiner which has a single output. When a single transistor fails in such an amplifier the output is reduced by an amount which depends upon the number of transistors being combined. This amount is shown in Figure 3.6, as a function of the number of transistors. It is 1.2 dB for an eight transistor amplifier. This is more loss than can be

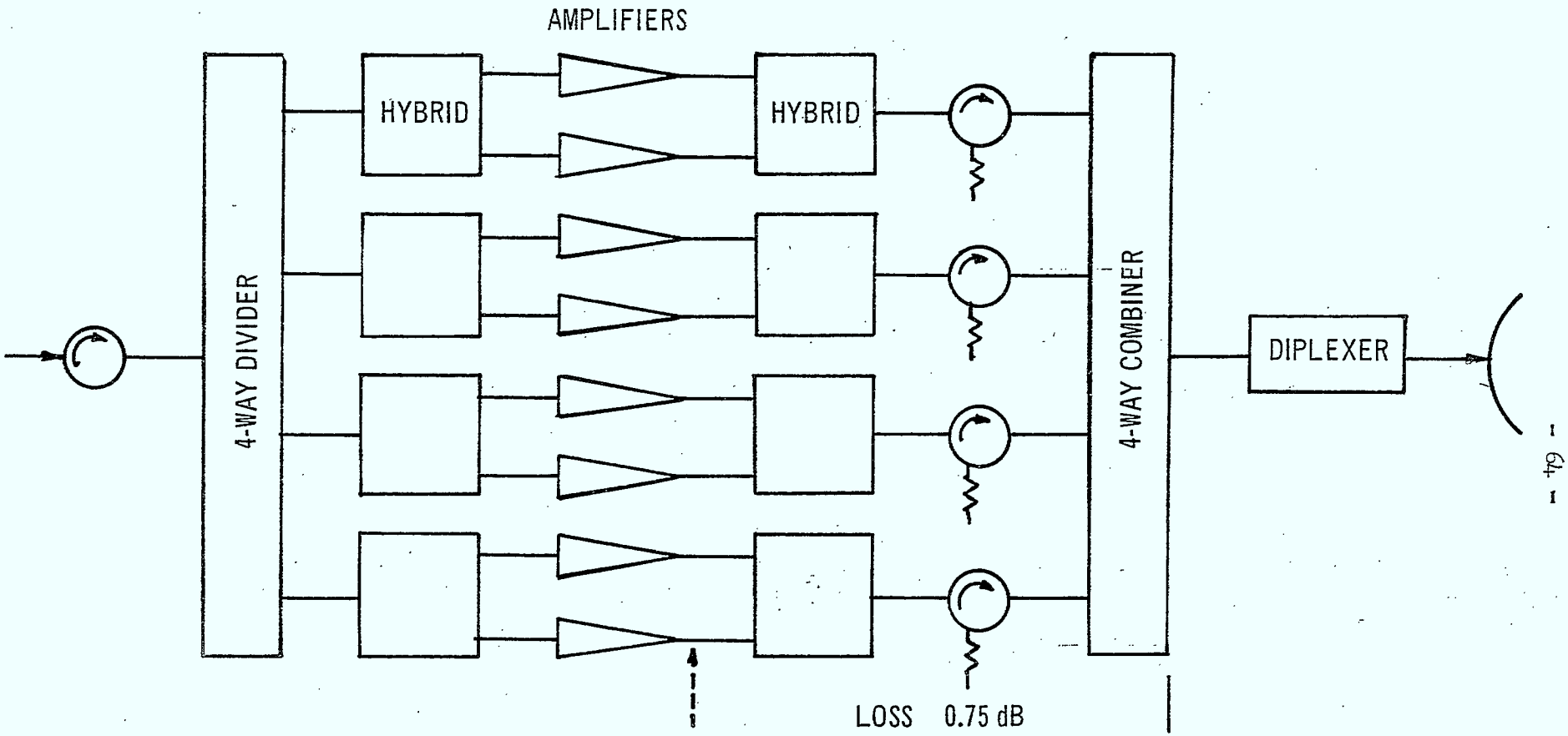

Figure 3.5 – An Eight-Way Power Combiner Using Hybrids

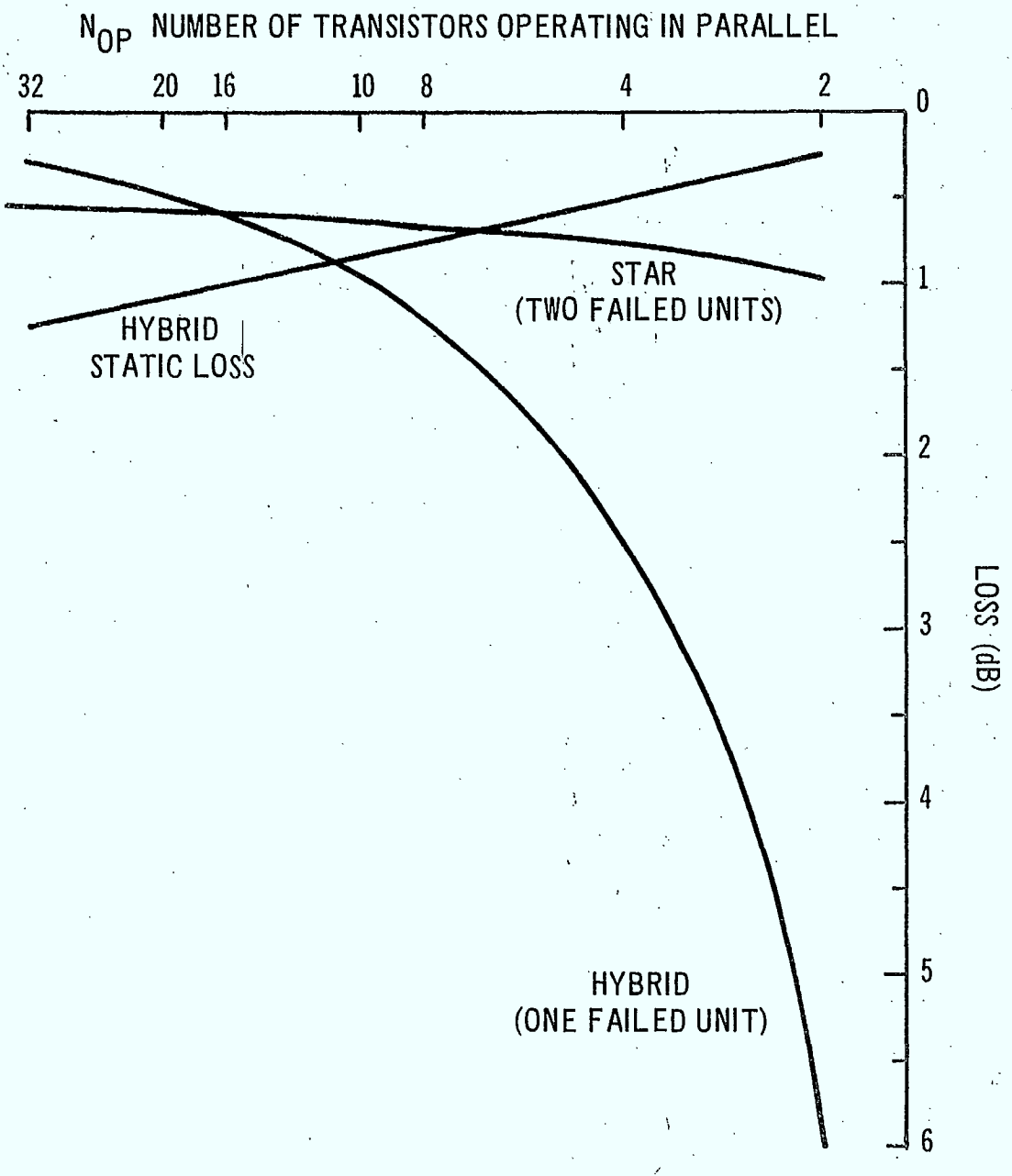

Figure 3.6 – Losses Associated with Star and Hybrid Combiners

tolerated so redundant units must be switched in as soon as the first transistor fails. This can be done by substituting the complete amplifier or by substituting individual transistors as they fail. This in general takes twice as many transistors as are actually operating at any one time. The static loss also increases as the number of operating transistors increases due to the increased number of hybrids required. The static loss is also plotted in Figure 3.6 assuming that .25 dB loss is added due to hybrids and isolators every time the number of transistors is doubled.

3.4.3 Star Combiner

The star combining network is shown schematically in Figure 3.7. The transistors are arranged in a circle and connected by quarter wave lines to the output transmission line at the center. The number of transistors around the circle consists of the number of operating transistors plus the necessary spares. The spare transistors are turned off until such time as one of the operating transistors fails. Then the failed component is turned off and one of the spare transistors is turned on. This returns the amplifier to full power except for the mismatch which may be introduced by the failed unit.

If the total number of transistors is N then the quarter wave lines have impedances such that the low output impedance of the transistor is transformed to NZ_o where Z_o is the impedance of the output line from the center. When the N lines are combined in parallel then the combined impedance is just Z_o. The resistances joining the transistor outputs are selected to minimize the mismatch caused by the spare transistors and the transistors that have failed. When all transistors are operating in phase the resistors carry

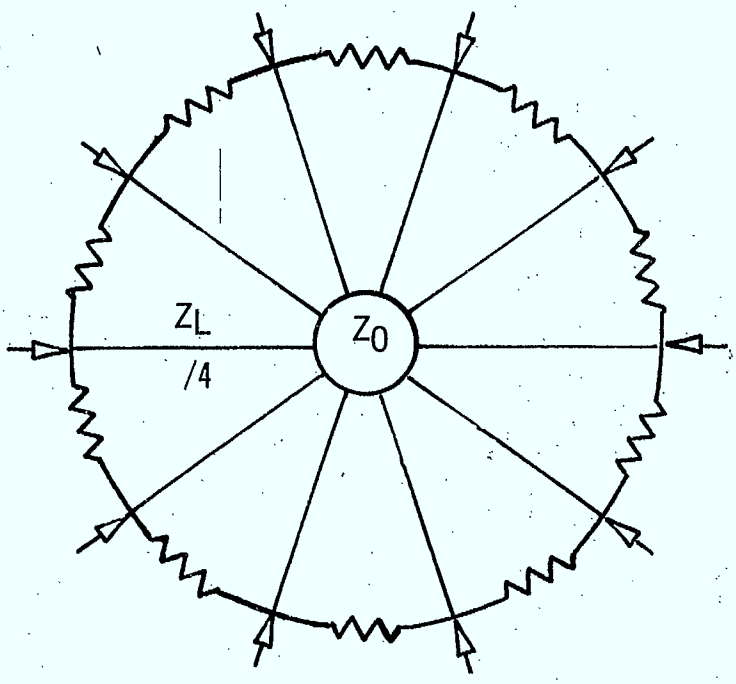

Figure 3.7 – A Star Combining Network with 10 Terminals

no current and dissipate no power. When a transistor fails by shorting the transformed impedance is infinite and a mismatch occurs at the output line. In addition, the transistors adjacent to the failed unit dissipate power in the resistors. When a transistor fails open it will present a high impedance. The resistors then form the source impedance. Thus decreasing the resistance reduces the mismatch for the spare transistors or transistors failed open and increases the mismatch for units that fail shorted. It is necessary to select resistance values and/or impedances between the transistors which minimize the losses under all conditions. This is a very complex problem and depends upon the number of transistors in the ring and the number of these which are spare. This problem has not been solved but some indication of trends can be obtained if it is assumed that the resistors R_L are pure real, and that the output impedance for an open or a spare transistor is controlled by the resistors and is equal to $R_L/2$. Then when a transistor fails open there is no change in output power and when a transistor fails short there is a mismatch at the output line and also in adjacent transistors. The overall loss can be further minimized by matching initially with some of the spare transistors replaced by shorts. This calculation has been carried out for the case of two spare transistors and a variable number of operating units N_{op}. The optimum resistance under these assumptions is given by

$$R_L = Z_{op}/\left(-\tfrac{1}{4}+\tfrac{1}{2}\sqrt{\tfrac{1}{4}+\frac{2}{N_{op}}}\right)$$

where Z_{op} is the output impedance of an operating transistor.

The minimum loss which corresponds to this resistance is given in

Figure 3.6 as a function of N_{op}. In addition to this loss caused by sparing a static loss would also occur with the star but it would be nearly independent of the number of transistors involved.

An examination of Figure 3.6 shows that as a general rule a hybrid combiner is better if the number of transistors is low and the star is better if the number is high. The cross over point appears to be for eight operating transistors. This is close to the number of transistors anticipated at 400 MHz, and even at 1.5 GHz the amplifier could be run with 8 rather than 5 parallel devices. This would suggest the use of a hybrid combiner rather than a star, however other advantages of the star must be considered. The star configuration incorporates an ideal sparing arrangement in that each spare may be substituted for any failed unit and every spare may be used before the amplifier must be considered failed. This is evident in Table 3.4 where the 7 and 8 year reliability figures are quoted for the devices in a number of star configurations and for an eight device and four device hybrid combiner amplifier. These figures have been calculated for a failure rate of .44 per 10^6 hours corresponding to a junction temperature of 110°C. It is seen that reliabilities obtained with a star configuration using one spar are equal to a hybrid configuration with a complete redundant amplifier. In addition the star may have another advantage, that of changing the operating level either up or down by switching in some of the spare units or switching out some of the operating units. In the case of the hybrid combiner there are no spare units to be turned on and the penalty incurred by turning units off is expected to be greater than for the star.

In the present system a star combiner is assumed although it is recognized that considerable development is required to fully evaluate its capabilities.

TABLE 3.4 - Reliability Estimates for Devices in Various Power Output Amplifiers at a Junction Temperature of 110°C.

Configuration	Number of Devices		Reliability	
	Active	Passive	7 Years	8 Years
Star	5	1	.990	.987
Star	6	1	.986	.982
Star	6	2	.999	.998
Star	7	1	.982	.977
Star	7	2	.998	.997
Star	8	1	.977	.971
Star	8	2	.998	.997
Hybrid	8	8	.962	.952
Hybrid	4	4	.989	.986

3.5 Power Amplifier Performance

3.5.1 Beam Power Triode Amplifier

Sufficient information is available on a conduction cooled power triode (RCA type 8828) to allow it to be evaluated as an output device in the transponder of the 400 MHz satellite system. Conduction cooling is by means of a BeO block approximately 0.83 sq. in. in area and .44 in. thick. Thermal conduction for BeO is 3 watts/^{o}C for unit area and unit thickness giving the thermal resistance as .18^{o}C/W.

The two tone intermod level is also specified for this tube at -30 dB in Class A operation. The corresponding efficiency is approximately 33% including heaters. For the 400 MHz satellite the end of life array power available for the output amplifier is 458 watts. With the expected efficiency for the tube this gives a radiated power of 150 watts and a dissipation of 300 watts. The radiated power of 150 watts is approximately half of that required for maximum channel capacity resulting in a satellite capable of only about half the maximum number of channels. The thermal model for a single tube dissipating 300 watts in shown in Figure 3.8. It is seen that if the mounting flange is kept below 100^{o}C the plate temperature will not exceed 155^{o}C. At this plate temperature and with the heater voltage reduced to 90% of nominal, the Mil HDBK-217A gives failure rates of one in 10^{6} hours. This is a reasonable failure rate, however, the wear-out life of the cathode surface is not defined. Because of experience with TWT's in space it is expected that the cathodes in beam power tubes would also survive the required length of time. However because of the low efficiency for Class A operation, tubes are not considered further.

3.5.2 Transistor Power Amplifier

The procedure for derating transistors and the corresponding reliability expected from the device is given in the handbook MIL HDBK-217A. The reliability is assumed to depend entirely on the transistor junction tempera-

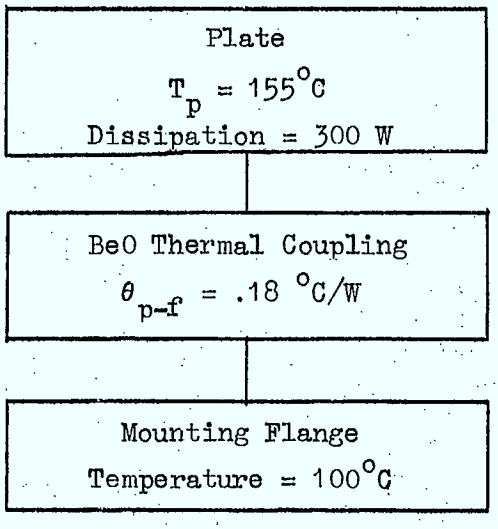

Figure 3.8 - Thermal model for a conduction cooled beam power tube operating Class A at 400 MHz.

ture and is related to it by means of a normalized junction temperature T_n by the equation

$$T_n = (T_j - T_s)/(T_{jmax} - T_s)$$

where T_j is the junction temperature

T_s is the case temperature at which power derating begins

T_{jmax} is the maximum rated junction temperature.

The reliability is related to T_n by a graph in the handbook and T_j is related to the device dissipation by the equation

$$T_j = T_c + \theta_{j-c} \times P_j$$

where T_c is the anticipated maximum case temperature

P_j is the average power dissipation

θ_{j-c} is the thermal resistance from junction to case.

The manufacturers data sheet gives the maximum value of θ_{j-c} for class C operation. For biased operation the temperature across the chip becomes nonuniform and it is necessary to use a higher value of θ_{j-c} corresponding to the highest expected hot spot temperature. This necessitates operation with a lower value of junction dissipation than for class C operation. The value of θ_{j-c} can be determined from the derating curves for biased operation.

The RF power generated by the device can be related to the dissipation once the efficiency and the power gain are determined. This relation is given by the equation

$$P_j = P_o \left(\frac{1}{\eta} + \frac{1}{G} - 1 \right)$$

where P_o is the RF output power

η is the efficiency (P_o/P_{dc})

G is the gain (P_o/P_{in})

Calculations have been carried out for representative transistors for which sufficient data has been available and extrapolated to the mid 1972 period. This has been done for both 1.5 GHz and 400 MHz and for class C and for class A operation. The results are given in Table 3.5 for different junction temperatures and for an assumed case temperature of 55°C. Two efficiencies are shown for each configuration, i.e. 25 and 30% for class A operation and 40 and 45% for class C except that at 400 MHz class C operation is much more efficient and efficiencies of 60 and 70% are used.

The figures in Table 3.5 for power output have been used to generate Table 3.7. In Table 3.7 are shown normal and eclipse operation for both 400 MHz and 1.5 GHz. Starting with the required EIRP and an assumed antenna gain the required number of simultaneously operating devices (Class A) are calculated for the various conditions. It is seen that at the required junction temperature of 110°C the number of devices in parallel is 65 at 400 MHz and 19 at 1.5 GHz. Even at a junction temperature of 150 °C (about as high as one can consider going) the numbers are 37 and 11 respectively. In addition, redundant units must be incorporated for reliability. It is considered impractical, however, to consider power amplifiers with this number of paralleled devices.

Turning to class C operation and 110°C junction temperature the number of transistors required is 8 for 400 MHz and 5 for 1.5 GHz. This is a more manageable number of parallel units so class C operation must be considered further.

TABLE 3.5 - Maximum Power Generated per Device in watts to Maintain Junction Temperature (T_J) Below Specified Value.

		T_n		.1	.2	.3	.4	.5
		T_J °C		110	120	130	140	150
		Failure rate $\times 10^6$	RCA	.44	.625	.89	1.25	1.77
			MIL HDBK 217A	.28	.39	.51	.65	.82
		Eff.	$\frac{1}{\eta} + \frac{1}{G} - 1$					
Class A 1.5 GHz 10 Volts $T_c = 55°C$	$P_J = (T_J - T_C)/\theta_{J-C}$			2.37	2.8	3.23	3.66	4.09
	TA 7994 $\theta_{J-C} = 23.3°C/W$	25	3.1	.765	.903	1.04	1.18	1.32
		30	2.43	.975	1.15	1.33	1.51	1.69
	Projected Early 1972 2.25 × TA 7994	25	3.1	1.72	2.03	2.34	2.66	2.97
		30	2.43	2.2	2.59	3.0	3.40	3.8
Class C 1.5 GHz $T_c = 55°C$	P_J			6.47	7.65	8.82	10.0	11.2
	TA 7994 $\theta_{J-C} = 8.5°C/W$	40	1.6	4.05	4.79	5.5	6.25	7.0
		45	1.32	4.9	5.8	6.7	7.6	8.5
	Projected Early 1972 2.25 × TA 7994	40	1.6	9.1	10.8	12.4	14.1	15.8
		45	1.32	11.0	13.0	15.0	17.0	19.1
Class A 400 MHz 10 Volts $T_c = 55°C$	P_J			7.34	8.67	10.0	11.4	12.7
	TA 7706 $\theta_{J-C} = 7.5°C/W$	25	3.2	2.29	2.71	3.13	3.56	3.97
		30	2.68	2.74	3.23	3.74	4.25	4.75
	Projected mid 1972 1.6 × TA 7706	25	3.2	3.67	4.34	5.0	5.7	6.35
		30	2.68	4.38	5.17	5.97	6.8	7.6
Class C 400 MHz $T_c = 55°C$	P_J			15.7	18.6	21.4	24.3	27.1
	TA 7706 $\theta_{J-C} = 3.5°C/W$	60	.87	18.0	21.4	24.5	28.0	31.0
		70	.63	25.0	29.5	34.0	38.0	43.0
	Projected mid 1972 1.6 × TA 7706	60	.87	29.0	34.0	39.0	45.0	50.0
		70	.63	40.0	47.0	54.0	61.0	69.0

TABLE 3.6 - Loss Budget

	400 MHz	1.5 GHz
Rotary Joint	-	.35 dB
Transmission Line	.1 dB	.1 dB
Duplexer	.3 dB	.3 dB
Filter	.5 dB	.5 dB
Switch	.35dB	-
Combiner	.75dB	.75 dB
TOTAL:	2.0 dB	2.0 dB

TABLE 3.7 - Performance of Satellites with Various Output Power Amplifiers (Projected mid 1972).

Frequency		400 MHz	400 MHz	1.5 GHz	1.5 GHz	2.5 GHz	2.5 GHz	2.5 GHz	2.5 GHz
Device		TR	TR	TR	TR	TR	TR	TWT	TWT
Operation		normal	eclipse	normal	eclipse	normal	eclipse	normal	eclipse
EIRP dBW		41.2	32.75	37.5	37.5	37.5	37.5	37.5	37.5
Antenna Gain dB		18.7	18.7	23.5	23.5	25.5	25.5	25.5	25.5
Output Power dBW		22.5	14.05	14.0	14.0	12.0	12.0	12.0	12.0
Generated Power	dBW	24.5	16.05	16.0	16.0	14.0	14.0	14.0	14.0
	Watts	282	40.2	39.8	39.8	25.1	25.1	25.1	25.1
Class A	EFF Trans = 30% EPS = 90%	.27	.27	.27	.27				
	DC Power	1040	149	148	148				
	Power/Device T_J = 110°C	4.38	4.38	2.2	2.2				
	Number	65	10	19	19				
	Power/Device T_J = 150°C	7.6	7.6	3.8	3.8				
	Number	37	6	11	11				
Class C	Back-off dB	.6	.6	.6	.6	.6	.6	2.5	2.5
	Class C Eff.%	80	80	45	45	35	35	31	31
	EPS Eff. %	90	90	90	90	90	90	90	90
	DC Power	450	64	113	113	91.7	91.7	160	160
	Power/Device T_J = 110°C	40.0	40.0	9.0	9.0				
	Number	8	1	5	5				
	Power/Device T_J = 150°C	69	69	15.8	15.8				
	Number	45	1	3	3				

It has been shown in Section 3.3 in the discussion of intermod that low intermod levels can be obtained with good efficiencies. This requires a small bias current and some detuning from the Class C power condition such that the loss in efficiency is of the order of 0.6 dB. In Table 3.7 the class C efficiency at 400 MHz is shown as 80%. This is presently quoted for class C operation at this frequency. The detuning brings this down to 70% and the power conditioner reduces this to 63% over all. With this type of output power amplifier maximum channel capacity can be obtained during normal sunlight operation at 400 MHz on a three axis stabilized spacecraft. However, during eclipse only about 18% channel capacity can be obtained.

At 1.5 GHz a class C efficiency of 45% is shown requiring 113 watts of DC power for the output amplifier. An efficiency of 45% is already being attained at 1.5 GHz, however, there is adequate weight capability at 1.5 GHz and additional power can be obtained if required.

3.5.3 2.5 GHz Transponder Considerations

Also included in Table 3.7 are two examples of operation at 2.5 GHz. The first is a class C transistor amplifier similar to that discussed for 400 MHz and 1.5 GHz. The second is a TWT operated with 2.5 dB of back-off.

To obtain the performance for the TWT transponder the solar array is increased in size to give the extra DC power required for the output amplifier. In addition a higher antenna gain is assumed which is accomplished with the same antenna aperture as at 1.5 GHz. The extra gain is obtained by means of an elliptical ground coverage pattern rather than the circular pattern proposed for 1.5 GHz. With these two changes the total EIRP during sunlight operation would

meet the maximum requirements. In addition, sufficient weight margin exists to obtain approximately 100% eclipse operation. In the case of the transistor amplifier maximum channel capacity can be obtained easily during both normal and eclipse operation. The required DC power for the output amplifier is 92 watts. This is less than that required at 1.5 GHz because of the higher antenna gain at the higher frequency. The specified class C efficiency of 35% is presently quoted by some manufacturers.

While very little work has been done at 2.5 GHz, it seems apparent that with either a TWT or a transistor amplifier a viable satellite can be configured at 2.5 GHz with full channel capacity during both normal and eclipse operation.

3.5.4 Heat Sink Requirements

The number of transistors has been based on a 55°C case temperature, however since only integral numbers of transistors are possible there is some extra capability over and above that indicated in Table 3.7. This can be used to ease the problem of dissipating the heat generated by the transistors. Maintaining the junction temperature at 110°C the maximum case temperature can be determined. Assuming a mica insulator between the case and the heat sink the maximum tolerable temperature for the heat sink can be calculated.

The thermal characteristics of one transistor for each of the two frequencies are shown in Figures 3.9 and 3.10. The maximum permissible temperature for the heat sink is very close to 50°C for both frequencies. It is considered to be a reasonable thermal problem to maintain the heat sink at a temperature less than 50°C.

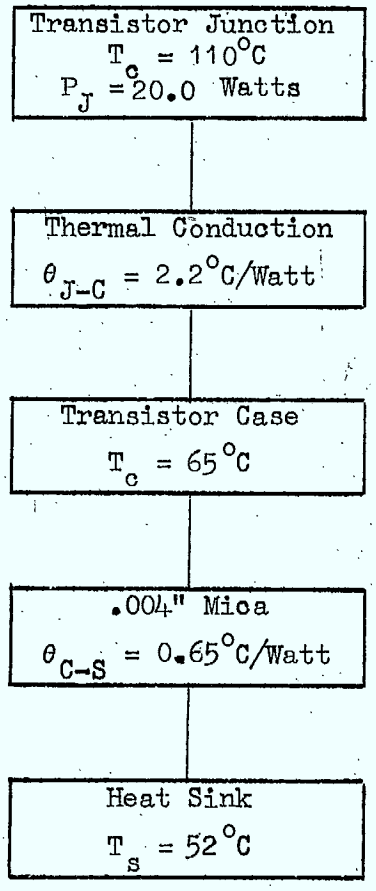

Figure 3.9 - Thermal design of a 400 MHz Class C transistor.

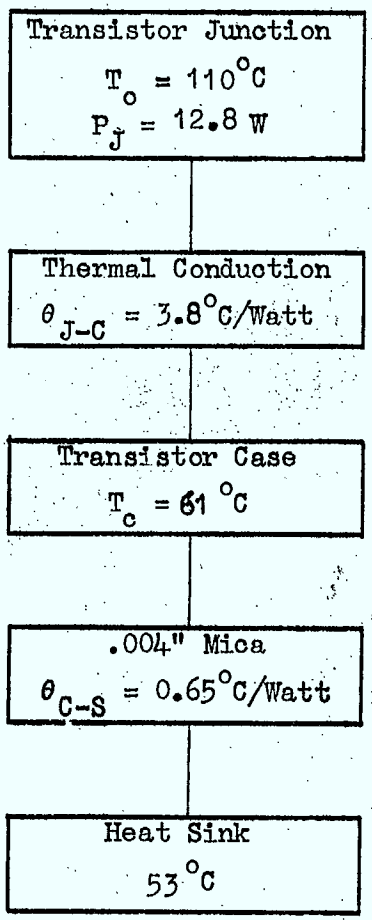

Figure 3.10 - Thermal design of a 1.5 GHz Class C transistor.

During eclipse operation the 1.5 GHz system operates at the same power level and therefore maintains approximately the same temperature. For the 400 MHz system the eclipse operation is reduced to 1/5 of the maximum capacity which maintains a temperature determined by the fourth power of the temperature. That is

$$\frac{T_{min}}{T_{max}} = (.2)^{\frac{1}{4}}$$

giving the minimum temperature during eclipse of $-57^{\circ}C$.

3.6 Proposed Transponder Configurations

The block diagrams shown in Figures 3.11 and 3.12 represent the proposed transponder configurations for 400 MHz and 1.5 GHz respectively. Redundant elements are not shown separately but are included in each individual block. It is considered that active units in the transponder chain are fully protected by cross-strapped redundant units. The receiver front end is an uncooled paramp. with a noise temperature of $75^{\circ}K$. Resistive losses in the feed line of 1.6 dB plus earth radiation brings this figure up to about $290^{\circ}K$. The transponder is all solid state using transistor oscillators and amplifiers and a diode frequency converter. The transponder at 400 MHz includes a separate low power amplifier for eclipse operation. Operation is switched from the main amplifier to the eclipse amplifier at the beginning of the eclipse and is switched back again at the end of eclipse. This is considered necessary because of the very large difference between the eclipse capability and the sunlight capability for this satellite. On the 1.5 GHz transponder, a rotary joint is required to transmit the signals

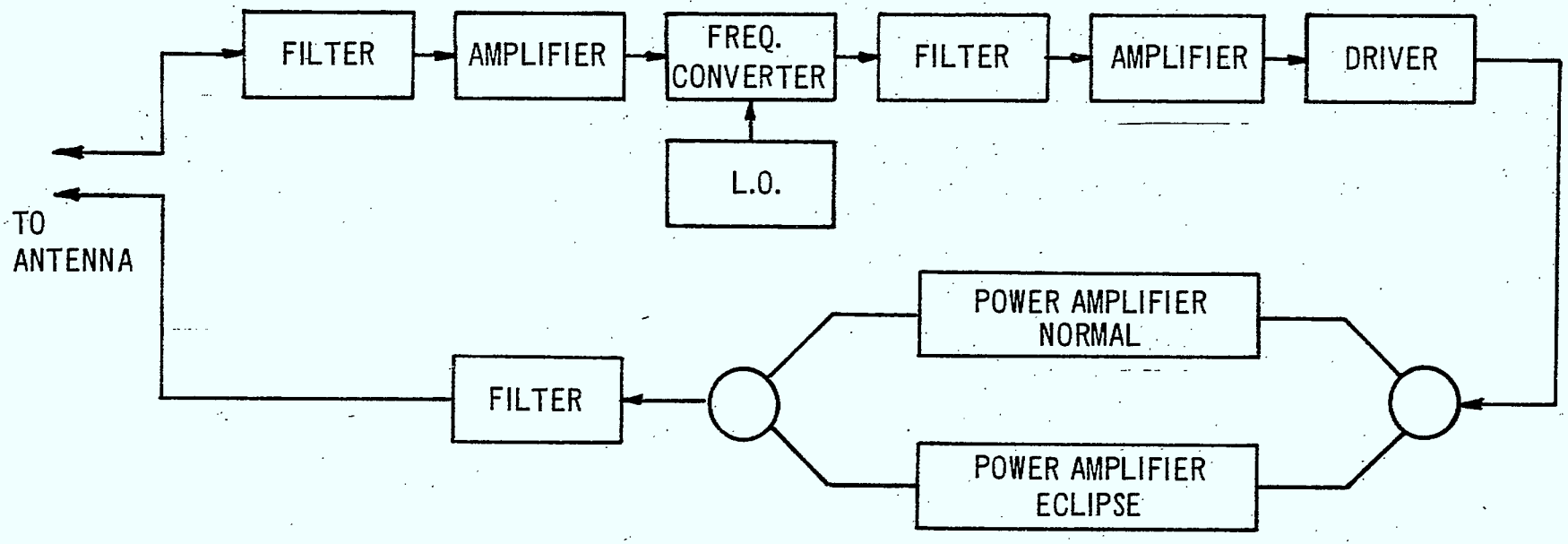

Figure 3.11 – Block Diagram of the 400 MHz Transponder

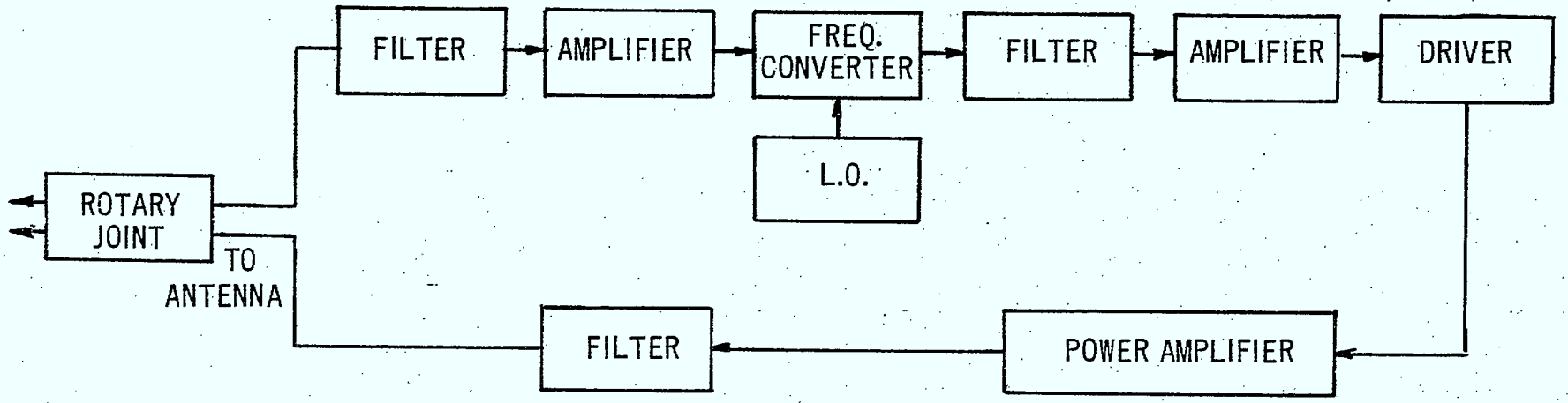

Figure 3.12 – Block Diagram of the 1.5 GHz Transponder

1.5 GHz Transponder	
Type	Single Frequency Conversion
Operation	F.D.M.A.
Design	All solid state
Input	Uncooled paramp.
Power Amp.	Multiple Parallel devices
Combining Network	Star configuration
Output power	14.0 dBW
Eclipse	100% capacity

400 MHz Transponder	
Type	Single Frequency Conversion
Operation	F.D.M.A.
Design	All solid state
Input	Low Noise Amp.
Power Amp.	Multiple parallel units
Combining Network	Star configuration
Power output	21.5 dBW
Eclipse	18% capacity with switched in output amp.

Table 3.8 - Specification of the Transponder Subsystems.

to the despun antenna. These are the only difference in concept between the transponders at the two frequencies. Subsystem specifications for the two transponders are given in Table 3.8.

A transponder for a 2.5 GHz spin stabilized satellite would be the same as the 1.5 GHz transponder.

REFERENCES

1. Hilling, H.E., and Salmon, S.K., "Intermodulation in Common-emitter Transister Amplifiers", Electronic Engineering, July 1968, pp. 360-364.

2. Chang, Z.F., and Locke, J.F., "Use of the RCA-2N6093 HF Power Transistor in Linear Applications", RCA Application Note AN-5491.

3. Thomas, L.C., "Broadband Linearization of Transistor Amplifiers", 1967 International Solid State Circuits Conference Philadelphia, Digest of Technical Papers, pp. 88-89.

4. Boag, J.C., and Newby, E., "Intermodulation Distortion Measurements on a Microwave Class C Transistor", RCA Research Memorandum 300, August 11, 1971.

5. Lambert, W.H., "Second-Order Distortion in CATV Push-Pull Amplifiers", Proc. IEEE, Vol. 58, No. 7, pp. 1057-1062, July 1970.

6. Wilkinson, E.J., "An N-way Hybrid Power Divider", IRE Trans. on Microwave Theory and Techniques, p. 116, January 1960.

7. Bailey, R.L., et al, "An All-Transistor, 1-kilo watt, High-gain UHF Power Amplifier", 1969 International Microwave Symposium, Dallas, Texas, Digest of Technical Papers, pp. 149-153.

4. ATTITUDE CONTROL AND DESPIN SUBSYSTEMS

4.1 Three Axis Attitude Control System

4.1.1 Whecon System

The present attitude control system for the CTS satellite is the "Whecon" system. This system, which consists of a biased angular momentum wheel and offset roll actuated thrusters, gives three axis attitude control without the need for yaw sensing. This attitude control scheme was adopted for the CTS satellite after a detailed trade-off study among three other candidate systems; the three reaction wheel system, the double-gimballed momentum wheel system, and the single momentum wheel with magnetics.

While the Whecon system is quite well suited for a two year mission, as in the case for CTS, for longer life satellites this system will not be satisfactory. There are two major reasons why this is so. At the present time both catalytic thrusters and resistojets have a limited life expectancy proportional to the number of firings of about two to three years in the Whecon configuration. The weight of the fuel required for satellite lifetimes in excess of five years will make the Whecon control system undesirable for our purposes.

4.1.2 Double Gimballed Reaction Wheel Control System

For a long life satellite with three axis attitude control, it appears that a double gimballed reaction wheel system will be most suitable (Fig. 4.1). This is especially true, when reliable yaw sensing is not available, due to the gyroscopic stiffness provided by the momentum wheel. It has also been shown in the CTS attitude control trade-off study that this system is lighter

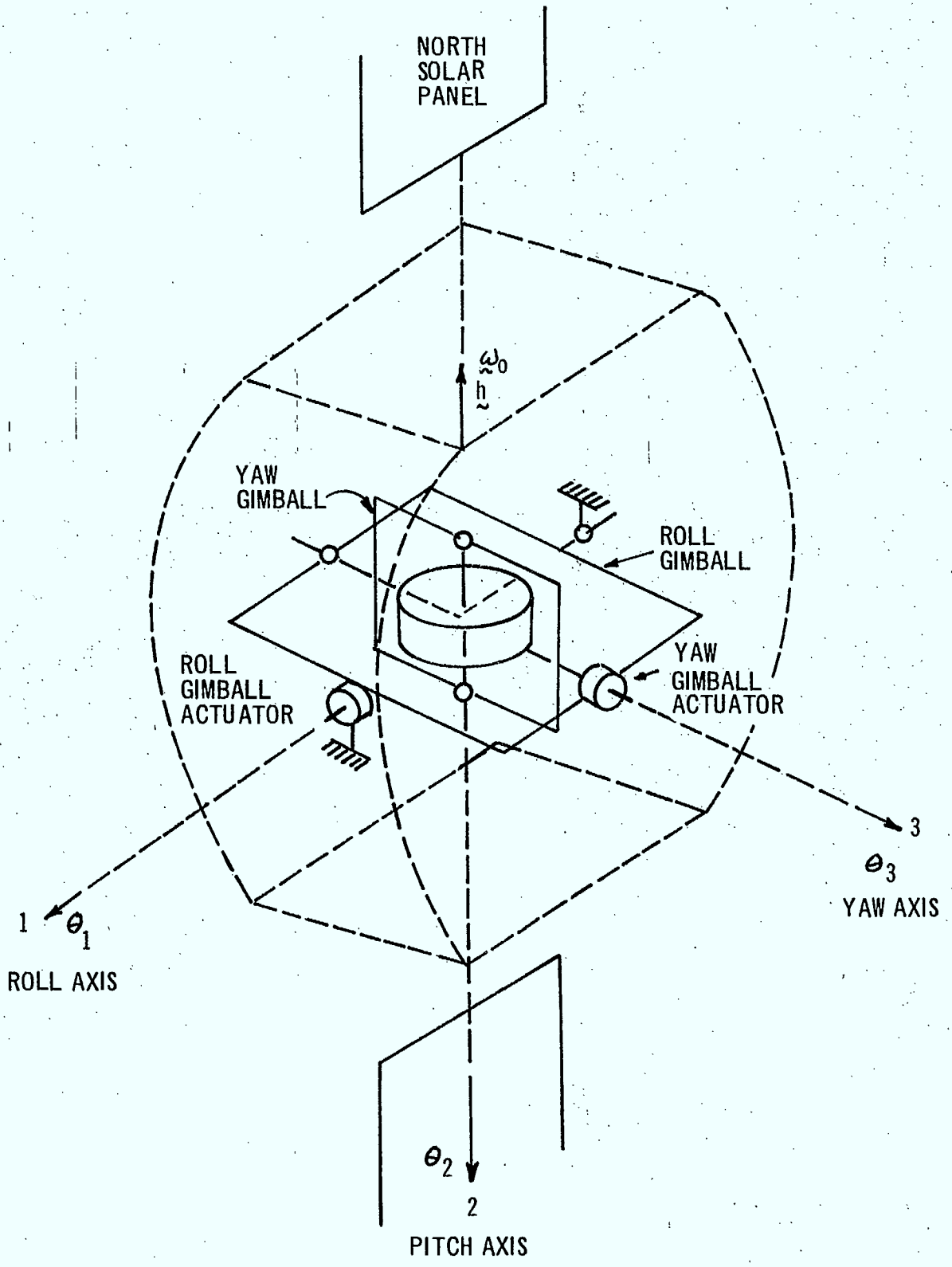

Figure 4.1 – Double Gimballed Reaction Wheel

than the three reaction wheel system as well as being more reliable.

The double-gimballed wheel system could use low thrust level ion engines or gas thrusters for station keeping and momentum desaturation. The wheel itself acts as an actuator in the pitch axis and, for small spacecraft displacements, provides control about pitch which is uncoupled from roll and yaw. Control in roll and yaw is provided by establishing a fixed angular momentum bias in the reaction wheel and steering this angular momentum in the roll-yaw plane by means of two gimbals.

The system is thus controllable in all three axis. The basic attitude sensor would either be of the horizon scanning type or a microwave interferometer which produces outputs of pitch and roll attitude. The roll attitude signal may be used to control both roll and yaw even if no yaw sensing is available on the satellite. Yaw control is obtained because of the roll-yaw coupling established by the wheel angular momentum bias. Yaw motion is thus coupled into roll such that yaw rate becomes observable from the roll output. Since the integration constant is unknown, the total yaw angle cannot be observed so that the control system can only provide rapid damping in the yaw channel. The steady-state yaw offset, due to external torques (mainly solar rotation pressure), is controlled by appropriate sizing of the bias angular momentum. This indirect yaw control avoids the necessity of employing star trackers or rate integrating gyro assemblies whose high cost and questionable reliability make them unsuitable for long life systems.

4.1.3 System Configuration

The double-gimballed wheel control system consists of the double-

gimballed momentum wheel, two gimbal actuators, and two gimbal angle transducers. There is also the attitude control electronics which contains the orbit motion decoupling computer as well as the system compensation networks and associated control electronics.

Roll and Pitch attitude information can be obtained either from a static earth sensor or a microwave interferometer. A careful trade-off study is necessary in order to decide between the two on the grounds of reliability, weight, and amount of ground control required for each system. A static sun sensor is provided in order to give yaw information, which will be required during east-west station keeping. Yaw information will only be available for two six hour periods per day.

4.1.4 Acquisition

The acquisition sequence for the spacecraft with the double gimballed reaction wheel system would be the same as that for the CTS spacecraft. This has a great advantage in that the software and experience developed for CTS would be directly applicable to the VHF satellite.

The satellite hardware required for acquisition and re-acquisition are a spinning earth sensor, a three axis rate gyro package, and a nutation damper, as well as the appropriate roll, yaw, and pitch thrusters.

4.1.5 Wheel Sizing Trade-offs

A significant weight saving results when the spacecraft pointing accuracy is relaxed from the demanding requirements of the CTS spacecraft. The size of the momentum wheel is completely specified by the maximum dis-

turbance torque and the maximum allowable yaw attitude error.

i.e. $$h = \frac{T_{d_{max}}}{\omega_o \psi_{max}}$$

where: h = wheel angular momentum

$T_{d_{max}}$ = maximum disturbance torque due to solar pressure

ψ_{max} = maximum allowable yaw error

ω_o = orbit frequency

In our case: $T_{d_{max}} = 1.5 \times 10^{-5}$ lb-ft.

$\omega_o = 7.29 \times 10^{-5}$ r/sec

$\psi_{max} = 7^o$

Therefore: $h = 1.68$ lb-ft sec.

This size angular momentum would allow us to choose a small reaction wheel of the size used in a three wheel control system.

4.2 Spin Stabilized Satellite

The attitude control system for the UHF satellite will consist of a spinning body with a despun antenna. Control system stability is ensured by having a favourable moment of inertia ratio as well as a nutation damper on the spinning section of the satellite. The despin system only gives closed loop control about the pitch axis. Roll and Yaw stiffness are provided by the tyroscopic motion of the spinning satellite. Attitude errors, which are allowed to build up to a dead band value, are corrected open loop by ground control of the axial thruster.

This type of attitude control system is quite standard and is presently being used on a number of successful satellites.

4.3 Attitude Control Subsystem Specifications

Parameter	Value
Spin Stabilized Satellite	
Beam Pointing Error	$\pm 0.5^{\circ}$ N-S (3σ) $\pm 0.5^{\circ}$ E-W (3σ)
Spin Rate Capability	75 - 125 RPM
Acquisition Time	< 15 min.
Attitude Sensing	Earth Sensor and Sun Sensors
Reliability	.920
Weight	40 lbs
Power	13.8 watts sunlight 13.8 watts eclipse
Three Axis Stabilized Satellite	
Beam Pointing Error	$\pm 0.5^{\circ}$ Pitch $\pm 0.5^{\circ}$ Roll $\pm 7^{\circ}$ Yaw
Attitude Sensing	Static Earth Sensor - Pitch and Roll Sun Sensor - Yaw
Reliability	.900
Weight	56 lbs
Power	30 watts sunlight 30 watts eclipse

5. OTHER SUBSYSTEM SPECIFICATIONS

The following pages summarize the performance specifications of those electronic subsystems not discussed in detail elsewhere in this volume. Data regarding other subsystems such as structure, apogee motor, etc. are found within the spacecraft budgets of Section 6.

POSITIONING AND ORIENTATION SUBSYSTEM

Spin Stabilized Satellite

Parameter	Value
Fuel	Monopropellant Hydrazine
No. of Tanks	4
Thrust Level	5 lbs
Axial Thruster	Pulsed - Attitude Control Continuous - N.S. Inclination correction
Radial Thruster	Pulsed - E-W Station Keeping
Dry Weight	24 lbs
Fuel Weight	125 lbs
Reliability	.970
Power	.5 watts sunlight .5 watts eclipse

Three Axis Stabilized Satellite

Fuel	Monopropellant Hydrazine
No. of Tanks	3
Thrust Level	Axial 5 lbs Radial 5 lbs Roll .1 lbs Pitch .1 lbs Yaw .1 lbs
Dry Weight	36.7 lbs
Fuel Weight	57.7 lbs
Reliability	.960
Power	.9 watts sunlight .9 watts eclipse

POWER SUBSYSTEM

Parameter	Value	
	Spinning Satellite	Non Spinning Satellite
Solar Cell Array		
Type	Body Mounted	2 Solar Sails
Power End of Life	217 watts	521 watts
Weight - Array Plus Array Structure	67 lbs	108.4
Battery		
Number of Batteries	2	2
Cycles	90 per year	90 per year
Max Normal Depth of Discharge	60%	60%
Weight	81 lbs	69 lbs
Power Control Unit		
Weight	19.8 lbs	19.8 lbs
Power	21 watts sunlight 8 watts eclipse	
Total Weight	167.8 lbs	197.2 lbs
Reliability	.950	.970

TELEMETRY SUBSYSTEM

Parameter		Value
RF Frequenoy		2250 MHz
EIRP		0 dBW
Modulation		PM
Encoding System		PCM
Tracking		By Residual Telemetry Carrier
Antenna:	Type	Belt Array
	Coverage	$\pm 20^{\circ}$
	Gain	0 dB within coverage
	Polarization	Linear N-S
Reliability		.965 5 years .945 8 years
Weight (Hardware)		13.9 lbs
Power		18 watts sunlight 10 watts eclipse

COMMAND SUBSYSTEM

Parameter		Value
Carrier Frequency		2060 MHz
Receiver Noise Figure		< 10 dB
Modulation		PM
Encoding System		PCM/FSK/AM
Antenna:	Type	Belt Array
	Coverage	$\pm 20^{o}$
	Gain	0 dB within coverage
	Polarization	Linear N-S
Reliability		.980 5 years .960 8 years
Weight		9.8 lbs
Power		3.6 watts sunlight 3.6 watts eclipse

6. SPACECRAFT BUDGETS

6.1 Three Axis Stabilized Spacecraft - Weight and Power

The configuration of the VHF satellite is based on the CTS spacecraft. Three axis stabilization is found necessary due to the amount of DC power required as well as the large size of the communications antenna.

In determining a weight budget for a three axis stabilized spacecraft the lifetime of the CTS spacecraft was extended with special attention being given to the pointing accuracy required by the VHF satellite. It quickly became evident that it would not be possible to extend the lifetime of the CTS spacecraft beyond five years within the present weight limitation of 1500 lbs. It appears that 1500 lbs is right at the lower weight limit of a three axis controlled communications satellite. Table 6.1 shows a weight and power breakdown for the case of the VHF satellite with a 5 year lifetime and 14% eclipse capability.

It can be seen that some means of reducing the spacecraft weight to meet the launch vehicle capability is necessary.

A possible solution would be to eliminate the fuel for the inclination correction. The fuel alloted to the N-S inclination control is based on the assumption of a 4 year dead band in the satellite "slot". By increasing the deadband to 5 years we can take advantage of the extra power available at the beginning of life in the solar array and thus manage without the need for any inclination control. This may result in a slight degradation of communications performance near the end of life time at 5 years.

The possibility of having some fuel for an inclination correction

TABLE 6.1 - Three Axis Stabilized Satellite - 5 Year Life

Subsystem	Weight lbs	Power		Notes
		Sun	Eclipse	
Structure	118.0	-	-	CTS Structure
Thermal	21.8	10.8	-	Modified CTS (take away SHF)
Electrical Distribution	24.3	4.0	4.0	CTS
TT&C Hardware	23.7	21.6	13.6	CTS (Excess capacity to be used to improve reliability for 5 years)
Antenna	7.0	-	-	CTS
Power Array	39.3	-	-	CTS 520 watts end of life
Array Structure	69.1	3.8	-	CTS
Power Cont. Unit	19.8	21.0	8.0	CTS
Battery	69.0	-	-	2 batteries
Attitude Control	56.0	30.0	30.0	Double gimballed reaction wheel
P&O Hardware	36.7	.9	.9	CTS
ABM Case	69.4	-	-	CTS
Fuel ABM	721.6	-	-	CTS
P&O E-W, ACQ. ATT.	57.7	-	-	CTS Attitude Study
N-S Inclination	18.6	-	-	4 year drift
Balance	15.0	-	-	CTS
Contingency 5%	75.0	9.2	5.7	
Sub-Total	1442.0	101.3	62.2	
Launch Vehicle Capab.	1500.0			
Payload	58.0			
Transponder	40.0	565.0	86.0	14% Eclipse Capability
Antenna	35.0			
Design Margin	-17.0			
Array Power Required		666.3		End of Life Power
Battery Power Required			148.2	

would still be there; if less fuel is used then predicted in the acquisition phase, or if any surplus weight at the time of launch, due to the 5% contingency, is used to fill up the fuel tanks.

The resultant saving of fuel is 18.6 lbs. This leaves a spacecraft design margin of + 1.6 lbs.

6.2 Spin Stabilized Satellite - Weight and Power

The configuration for the spin stabilized UHF satellite is based on the Canadian Domestic Communications Satellite and the CTS spacecraft. The relatively low power required, compared to the VHF configuration, allows us to go to a spin stabilized configuration with a despun antenna.

A number of significant weight savings are realized by going to a spin stabilized satellite. The main areas are:

(a) The simplicity of a body mounted solar array results in a large saving over the complex solar sail system of the three axis spacecraft.

(b) Thermal control in a spinning satellite is much simpler than in a non-spinning satellite.

(c) The attitude control system for the spinning satellite is much simpler and lighter than the complex three axis attitude control system. The hardware required for acquisition as well as the acquisition procedure is very much simpler for the spinning satellite.

(d) The Positioning and Orientation Control System is lighter mainly due to the lighter tanks which take advantage of the fact that the satellite is spinning.

Two major areas where the spinning satellite is more complex than the non-spinning configuration are:

(a) The requirement for a rotary joint to transfer the commu-

TABLE 6.2 - Spin Stabilized Satellite - 8 Year Life

Subsystem	Weight lbs	Power		Notes
		Sun	Eclipse	
Structure	90.0	-	-	86" diam., 55" long
Thermal	15.0	3.5	7.5	
Electrical Distrib.	17.0	4.0	4.0	
TT&C Hardware	23.7	21.6	13.6	CTS (modified)
Antenna	7.0	-	-	CTS
Power Array	67.0	-	-	252 watts end of life
Battery	81.0	-	-	2 batteries
Power Control Unit	19.8	21.0	8.0	CTS
Attitude Control	40.0	13.8	13.8	
P&O Hardware	24.0	0.5	0.5	Can. Dom. Com. Sat. Study
ABM Case	69.4	-	-	CTS
Fuel ABM	721.6	-	-	CTS
P&O EW-ACQ-Att.	50.0	-	-	
N-S Inclination	75.0	-	-	
Balance	6.0	-	-	2X CDCSS
Contingency 5%	75.0	12.6	11.1	
Sub-Total	1391.5	77.0	58.5	
Launch Vehicle Capab.	1500.0			
Payload	108.5			
Antenna & Structure	25.0			
Transponder	40.0	140.0	140.0	
Design Margin	+43.5			
Array Power Required		217.0		End of life power
Battery Power Required			198.5	

nications signal between the spinning satellite and the mechanically despun antenna.

(b) Due to the large size of the communications antenna, the antenna will have to be folded up during the launch and transfer orbit phase. Once the satellite is on-station the antenna will have to be deployed. While this would be quite simple in a non-spinning satellite, with the spinning satellite, a great deal more care will have to be taken while deploying the antenna so as not to upset the basic stability of the satellite.

6.3 Reliability

A reliability budget has been compiled (Table 6.3) giving reasonable estimates of the reliability that can be obtained for each subsystem. These estimates were made taking into account the information available from the Telesat study as well as the CTS reliability estimates. It should be possible to meet these estimates, with a realistic amount of redundancy, and still remain within the weight estimates shown in Tables 6.1 and 6.2. It can be seen that the reliability for the complete satellite in each configuration is about the same even though the satellite lifetimes are different. This is a reflection of the basic simplicity of the spin-stabilized configuration.

The estimates for the reliability for the communications subsystem are based on the information presently available on high power RF transistors. When more information on these devices is available it may be possible to achieve a higher reliability in this area.

Subsystem	Reliability	
	Three Axis (5 years)	Spin Stabilized (8 years)
Structure and Thermal	.995	.995
Electrical Distribution	.980	.960
Telemetry	.965	.945
Command	.980	.960
Power	.970	.950
Attitude Control	.900	.920
P&O	.960	.970
Communications	.900	.900
Total Spacecraft	.695	.685

Table 6.3 - Reliability budgets for the two spacecraft configurations.

7. PROGRAM COSTS-SPACE SEGMENT

In developing the budgetary estimates for the space segment of this system, a large number of assumptions have had to be made and some ground rules developed, the most important of which are discussed below.

(a) The costs are based on available data adjusted for factors considered to be program peculiar.

(b) The figures quoted are budgetary cost estimates excluding profits and incentives. The latter factors are too dependent upon the form of contracts and the contracting pattern to permit satisfactory estimation. As a rough order of magnitude these may be estimated at 10-15%.

(c) The estimates are based on a program which follows good commercial spacecraft practice procurements. In this regard it is assumed that the procurement is to a spacecraft performance specification and that prime contractor control is to that level. It is further assumed that no special financial or technical visibility or reporting is required.

(d) It is assumed that all the required technologies are available but that most subsystems require development to the extent that normal design reviews, breadboard and engineering models are required during the program. Thus, for example, the CTS technologies are considered as proven at the time of the program implementation but that no subsystem can be a direct reprocurement of an unmodified design. However, when appropriate the costs do reflect savings which result from off-the-shelf-units or devices where such savings commonly occur.

(e) The program is costed on the basis of a 24-30 month first launch ARO, with the second at an interval such as to phase with good continuity into the integration and test facility.

The basic program consists of the appropriate models: mechanical - thermal; engineering and prototype all within the nonrecurrent costs. For economy it has been assumed that the prototype is refurbished and tested to flight levels to act as launch back up to flights 2 and 4. (Launch 2 is back up on 1, 4 on 3). The reburbishing and retest cost estimate on the prototype is shown separately in as much as they are discretionary and likely to be implemented only on a launch or early failure.

(f) Cost estimates do not include duties, sales taxes or royalty payments. All figures are in Canadian dollars and do not permit unreasonable variations in exchange rates on units, subsystems or components likely to be of foreign origin.

(g) While every effort possible within the scope of this study has been made to develop accurate figures, the accuracy of the forecasts of costs, inflation and influence of other programs is such as to make these estimates liable to considerable error. Within these constraints and limitations it is felt that an overall accuracy of 10 to 20% has been achieved, with the expressed hope that the former is applicable to the total space segment costs, while the latter is more likely to apply to individual subsystem or phase costs.

Table 7.1 gives the cost estimates for the 1.5 GHz space segment while Table 7.2 gives those for the design at 300 MHz.

TABLE 7.1 - Spin Stabilized Satellite - Estimated Cost

Item	Non-Recurring	Prototype	Unit Flight S/C	Refurb. Proto	Non Phased	Total
System & Subsystem Eng.	2.5	.4	.2			
Communications	2.5	1.5	1.0			
Antenna	.75	.25	.2			
TT&C	.5	.55	.5			
AD&D	1.6	.9	.75			
Power	.8	.75	.6			
Elect. Dist.	.3	.15	.1			
P&O	1.5	.35	.3			
Thermal	.55	.2	.15			
Apogee Motor	.55	.2	.15			
Structure	.75	.5	.5			
Integration & Test	.4	1.5	1.0			
Range Ops			.15			
Program Manag.					4.5	
G.S.E.					2.5	
TOTAL COST	12.7	7.25	5.60	1.0	7.0	

TABLE 7.2 - Three Axis Stabilized Satellite - Estimated Cost

Item	Non-Recurring	Prototype	Unit Flight S/C	Refurb. Proto	Non-Phased	Total
System Eng.	3.0	.4	.2			
Communications	2.5	1.5	1.0			
Antenna	1.5	.5	.3			
TT&C	.5	.55	.5			
Attitude Control	2.0	1.0	.8			
Power	1.0	1.25	1.0			
Electrical Dist.	.3	.15	.1			
P&O	1.6	.4	.3			
Thermal	.75	.3	.2			
Apogee Motor	.55	.2	.15			
Structure	.8	.5	.5			
Integration & Test	.4	1.5	1.0			
G.S.E.					2.5	
Range Ops.			1.5			
Program Manag.					4.5	
TOTAL COST	14.90	8.25	6.20	1.0	7.0	

LKC
P91 .C654 U35 1971 v.2
UHF communications satellite
system : final report

TEM:

DATE DUE
DATE DE RETOUR

LOWE-MARTIN No. 1137

INDUSTRY CANADA / INDUSTRIE CANADA
208172

RCA